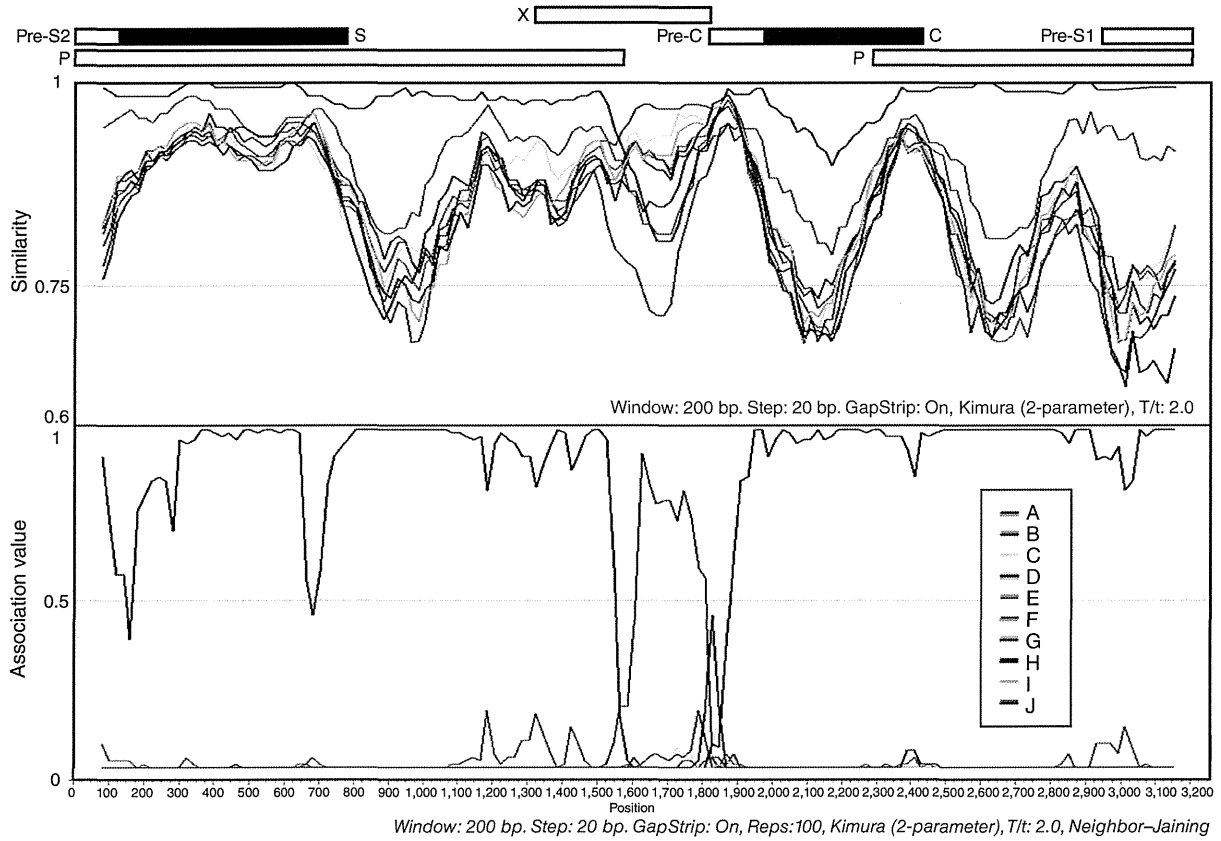

Figure 3 Nucleotide similarity comparison of the full-length sequence of the hepatitis B virus (HBV) strain isolated from case 2 in reference to previously reported HBV genotypes A–J. The parameters used for the analysis are shown at the bottom of the figure (200-bp window size, 20-bp step size, 100 bootstrap replicates, gap-stripped alignments and neighbor-joining algorithm).

were classified as genotype H according to full-length nucleotide sequence analysis, with an identity of 96.4% to 95.8% to each other, and as genotype B based on analysis of the nucleotide sequence between DR2 and DR1, with an identity of 96.9% to 95.8%, respectively. However, the nucleotide sequence between 2023 and 2262 nt in the precore/core regions showed no similarity to that of any previously reported HBV strains. In these regions, the C2-1 and C2-2 clones showed nucleotide sequences with an identity of 98.6% to each other, and the nucleotide divergences in comparison to strains of genotypes A–J ranged 9.6–30.0% in the C2-1 clone and 8.1–28.5% in the C2-2 clone (Table 1). A phylogenetic tree constructed based on these regions revealed that both strains may be classified into the novel cluster of HBV (Fig. 4b). Also, the amino acid sequence divergences from previously reported HBV strains ranged from 18.1% to 27.9% in the C2-1 clone and 17.1% to 26.9% in the C2-2 clone.

The nucleotide sequence data reported in the present study will appear in the DDBJ/EMBL/GenBank databases under accession number AB818694 for case 1, AB819065 for the C2-1 and AB819066 for the C2-2 strain.

DISCUSSION

IN THE PRESENT paper, the genotypes of the HBV strains isolated from 222 patients with acute and chronic hepatitis B were evaluated by EIA and/or PCR-INVADER assay, and HBV genotype A strains, commonly isolated in Africa, Europe and India, were found in 9.4% of the patients; genotype A strains were isolated from 50.0% of patients with acute liver diseases and 3.1% of patients with chronic liver diseases. These values were almost in line with those reported from other institutions in Japan.[11–13] HBV genotype A strains are known to be frequently isolated from patients with

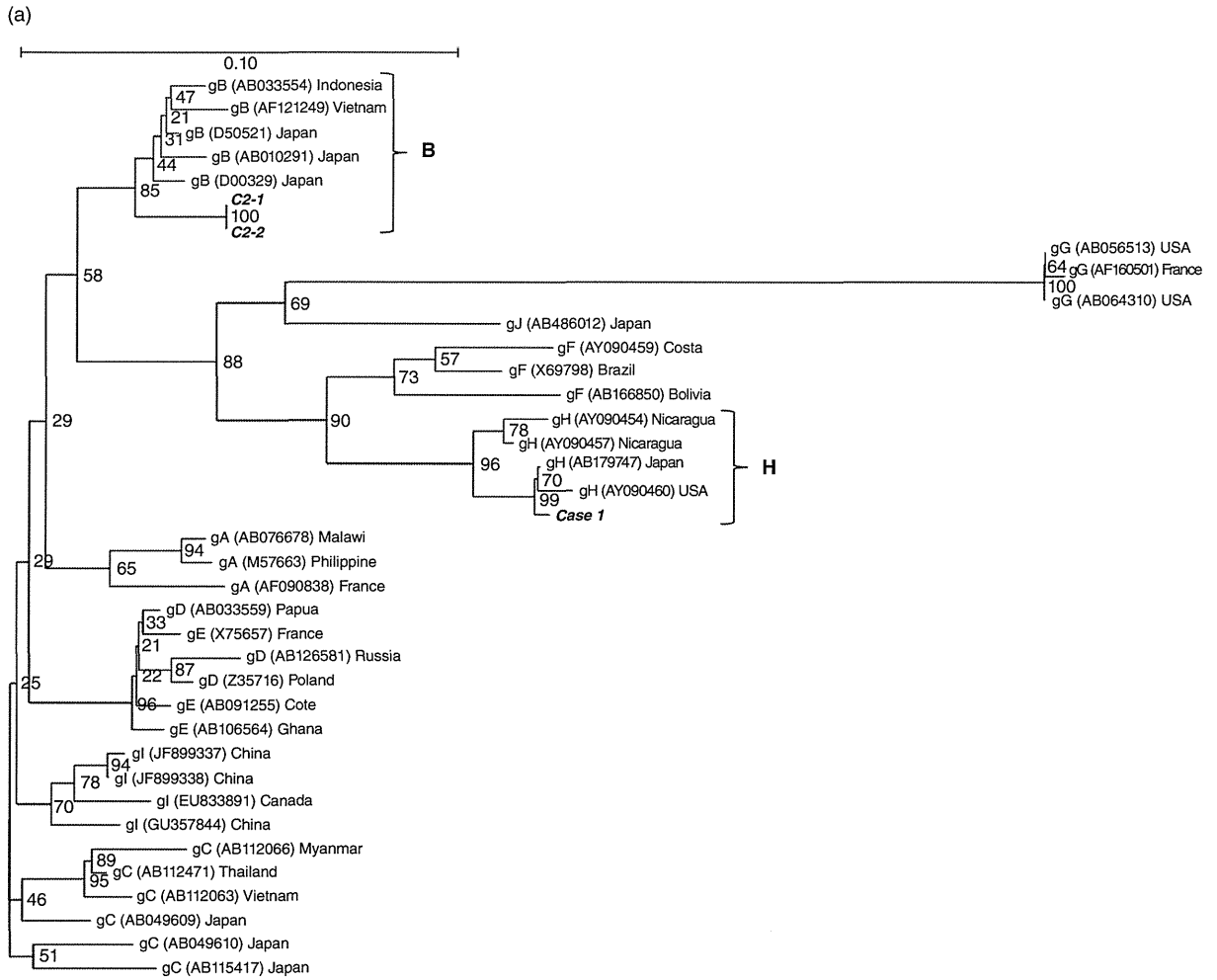

Figure 4 A phylogenetic tree constructed based on the sequence of the hepatitis B virus (HBV) strain isolated from case 2 in comparison with that of 35 reference strains. The bootstrap values are indicated at each tree root and the genotypes are on the right. The horizontal bar provides a genetic distance. The regions included in the analysis were: (a) nucleotide sequence between DR2 (1590 nt) and DR1 (1834 nt) in the X region, (b) between 2023 and 2262 nt in the precore/core region.

acute liver diseases caused by HBV, especially in urban areas as compared to the countryside,[29] suggesting that globalization and diversification of the sex industry may change the distribution pattern of the HBV genotypes in Japan, including in Saitama Prefecture, the area around our institution.

To our surprise, HBV genotype H strains, which are mainly prevalent in Central America, were isolated from two patients, one each with chronic and acute liver diseases. The HBV strain isolated from the patient with acute liver disease (case 1) showed a nucleotide sequence with 99.8% identity to the Thailand strain (EU498228), which has recently been reported to be isolated from Japan as well as Central America.[30] Considering that case 1 was a bisexual male with HIV co-infection contracted as a result of sexual activities with a number of unspecified Japanese partners, the HBV strain isolated from this patient may be resident in Japanese persons engaging in unusual sexual activities. On the other hand, HBV genotype A strains, especially the genotype A2/Ae strain, have been isolated increasingly frequently from patients with HBV and HIV co-infection.[31] These observations prompted us to postulate that HBV genotype H strains as well as genotype A

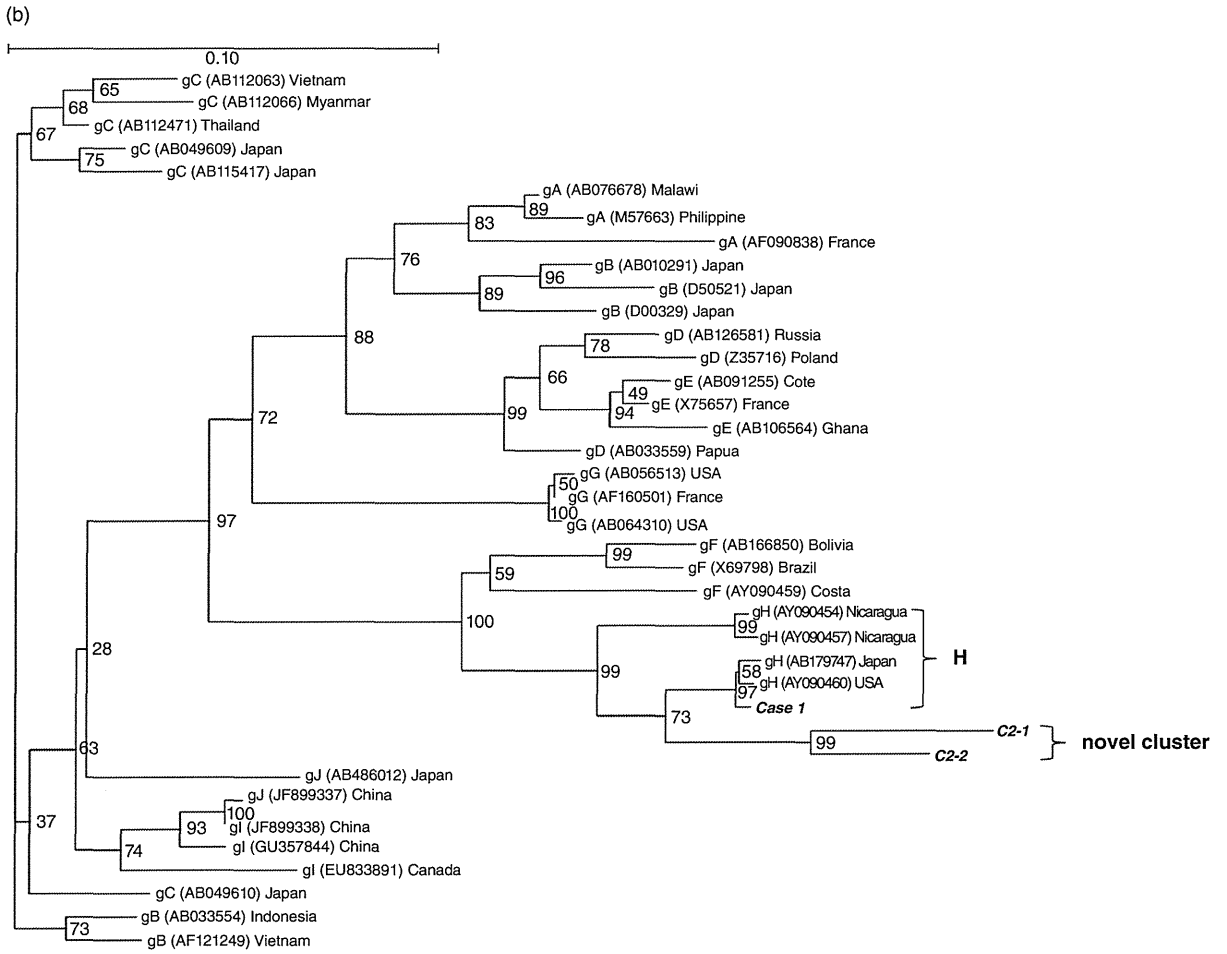

Figure 4 *Continued*

strains seem to spread among Japanese persons with unusual sexual habits. Previously, Tanaka *et al.* reported a HIV-infected patient in whom co-infection of both HBV genotype H and G strains was observed.[32] In case 1, however, co-infection of HBV genotype G strain was not detected.

It is noteworthy that HBV genotype H strains were isolated even from a Japanese patient with chronic liver disease (case 2), which showed recombination with a genotype B strain. The recombination breakpoint was estimated at positions 1590 and 1834 nt, located between DR2 and DR1 in the X region (Fig. 5): the nucleotide sequence in the X region of this strain showed an identity of 97.2% to that of genotype B strains in Malaysia (JQ027316) and Indonesia (JQ429079) despite the full-length nucleotide sequence showing 97.1% identity to a genotype H strain isolated from Mexico (AB375164). In the present study, nucleotide sequences were analyzed using two fragments (WA2 and gN2), suggesting that the possible recombination points exist in the overlapping regions of both fragments. However, the possibility that both genotypes B and H HBV strains existed as quasispecies in case 2 was neglected, because the sequences of the overlapping regions (1702–1780 and 1908–2081 nt) showed 100% identity between WA2 and gN2 fragments. It is well known that a HBV genotype B2/Ba strain, widely prevalent in Asian countries, shows nucleotide sequences identical to genotype C strains in the precore/core region due to the inter-genotype recombination

Table 1 Percentages of differences in the nucleotide and amino acid sequences of hepatitis B virus (HBV) strains isolated from case 2 (C2-1 and C2-2) and representative strains of genotypes A–J HBV

		Percentages of differences to representative HBV strains of genotypes							
		A (3)	B (5)	C (6)	D (3)	E (3)	F (3)	G (3)	H (4)	I (4)	J (1)
C1-1	Nucleotide	25.9–30.0	25.6–28.6	24.4–26.9	26.9–29.6	28.5–29.8	17.6–17.9	26.2–26.7	9.6–13.0	24.8–26.5	26.1
	Amino Acid	18.6–25.7	21.3–25.1	23.8–27.9	22.8–25.5	24.2–25.7	18.1–18.2	22.8–24.2	18.1–19.4	22.7–27.3	24.6
C2-2	Nucleotide	24.4–28.5	24.1–27.1	22.9–25.4	25.4–28.1	27.0–28.3	16.1–16.4	24.7–25.2	8.1–11.5	23.3–25.0	24.6
	Amino Acid	17.6–24.7	20.3–24.1	22.8–26.9	21.8–24.5	23.3–24.7	17.1–17.2	21.8–23.3	17.1–18.4	21.7–26.3	23.6

Values in parenthesis indicate the number of HBV strains.

between B and C strains.[33] Also, HBV strains developing as a consequence of the inter-genotype recombination between A and D, A and E, A and C, C and D, and C and G have been reported from Africa, Vietnam, Tibet and Thailand.[34–37] Moreover, recombination among HBV strains of the same genotype, the so-called intra-genotype recombination, has been proposed to occur especially in HBV genotype A, D, F and H strains.[38] However, HBV genotype H strains showing recombination with other genotype strains have not ever been reported. Considering the fact that the father of case 2 had lived in Brazil in his youth, the sequences of genotype H in case 2 strains might have originated in Brazilian strains. In Brazil, genotypes A and D HBV strains are predominantly distributed with frequencies of 49.5% and 24.3%, respectively, while genotype B HBV strains are only 2.9%.[39] Thus, the recombination event with the genotype B HBV strain might have developed following the emigration of his father to Japan. To clarify the area and era in which the recombination developed, the full-length nucleotide sequence of the HBV strain isolated from the elder brother of case 2 needs to be evaluated, but, unfortunately, the brother, receiving medical examination at another institution, rejected further viral genome analysis.

Although the mechanisms involved in the development of inter-genotype and intra-genotype recombination of the HBV genomes remains unclear, several observations reported in previous publications prompted us to postulate the "non-random pathway"; DR1 (1830 nt) in the X gene, a possible origin of viral replication, is considered to be a hot spot that may be responsible for recombination of HBV genomes among different strains.[40,41] Hino *et al.* reported, based on *in vitro* recombination assay, that HBV DNA fragments containing the region spanning DR1 increased the recombination events reproducibly in the presence of extracts from actively dividing HCC cells.[40] Also, Pineau *et al.* revealed that the integration sites of covalently closed circular HBV DNA were usually located in the nucleotide sequence between 1600 and 2000 nt, when the HBV genomes chromosomally integrated in the host genomes were evaluated in human HCC tissues.[41] These *in vitro* and *in vivo* observations were consistent with the results obtained from the analysis of the HBV strains isolated from case 2, showing that the genome of the HBV genotype B strains were integrated in that of the HBV genotype H strain between DR2 and DR1.

Hepatitis B virus strains isolated from case 2 were classified as quasispecies in accordance with the nucleotide sequence between 2023 and 2262 nt in the precore/

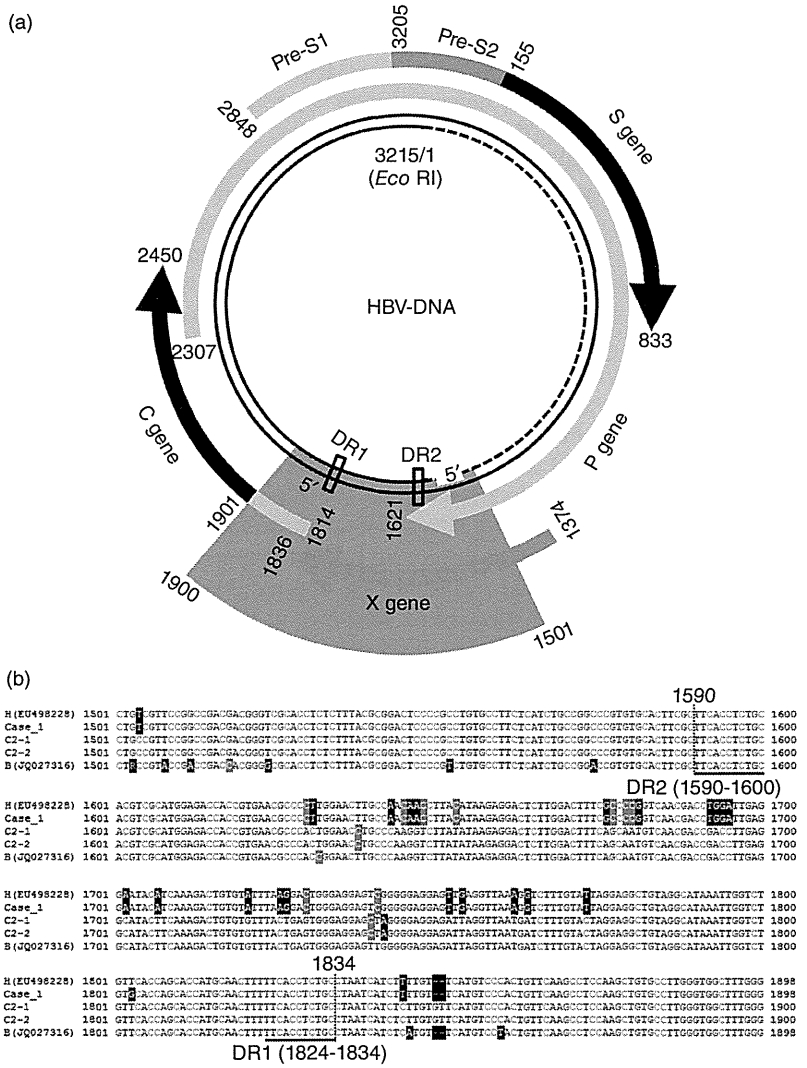

Figure 5 Hepatitis B virus (HBV) genome and the open reading frame. (a) The sequence region (shaded in red) includes the recombination breakpoint at position 1590 and 1834 nt, located between DR2 and DR1 in X region. (b) Nucleotide alignments over the sequences spanning 1501–1900 nt in case 1, C2-1, C2-2 and reference strains of HBV genotype H (accession no. EU498228) and B (JQ027316). Dashed lines at 1590 and 1834 nt represent the recombination breakpoint.

core regions. Thus, the nucleotide sequences were analyzed following cloning of the HBV genome, and two major clones, C2-1 and C2-2, were isolated. Neither clone showed any similarity to any of the previously reported strains in the precore/core regions, and a phylogenetic tree constructed based on these regions revealed that these strains may be classified into the novel cluster of HBV; sequence divergences of nucleotides in the range of 8.1–30.0% and of amino acid in the range of 17.1–27.9% as compared to previously reported genotype A–J strains. The possibility that inter-genotype recombination of the HBV genome between H and B strains may provoke mutation of the nucleotide sequence in the precore/core regions leading to development of a possible novel genotype HBV strain needs to be evaluated in the future.

In conclusion, HBV genotype H strains, which are prevalent in Central American countries, were isolated from Japanese patients with chronic as well as acute liver diseases. HBV strains isolated from the chronic liver disease patient showed recombination of the genome between genotype H and B strains, and no similarity was found in the nucleotide sequences of the precore/core regions in comparison with those of the previously reported HBV strains. Thus, globalization may promote development of a possible novel genotype of HBV through recombination between Central American and East Asian strains.

REFERENCES

1 Schiff ER. Prevention of mortality from hepatitis B and hepatitis C. *Lancet* 2006; **368:** 896–7.
2 Ganem D, Prince AM. Hepatitis B virus infection – natural history and clinical consequences. *N Engl J Med* 2004; **350:** 1118–29.
3 Perz JF, Armstrong GL, Farrington LA, Hutin YJ, Bell BP. The contributions of hepatitis B virus and hepatitis C virus infections to cirrhosis and primary liver cancer worldwide. *J Hepatol* 2006; **45:** 529–38.
4 Ikai I, Arii S, Okazaki M *et al.* Report of the 17th nationwide follow-up survey of primary liver cancer in Japan. *Hepatol Res* 2007; **37:** 676–91.
5 Umemura T, Ichijo T, Yoshizawa K, Tanaka E, Kiyosawa K. Epidemiology of hepatocellular carcinoma in Japan. *J Gastroenterol* 2009; **44** (Suppl 19): 102–7.
6 Fujiwara K, Mochida S, Matsui A, Nakayama N, Nagoshi S, Toda G. Fulminant hepatitis and late onset hepatic failure in Japan. *Hepatol Res* 2008; **38:** 646–57.
7 Sugawara K, Nakayama N, Mochida S. Acute liver failure in Japan: definition, classification, and prediction of the outcome. *J Gastroenterol* 2012; **47:** 849–61.
8 Oketani M, Ido A, Nakayama N *et al.* Etiology and prognosis of fulminant hepatitis and late onset hepatic failure in Japan: summary of the annual nationwide survey between 2004 and 2009. *Hepatol Res* 2013; **43:** 97–105.
9 Tiollais P, Charrnay P, Vyas GN. Biology of hepatitis B virus. *Science* 1981; **213:** 406–11.
10 Okamoto H, Tsuda F, Sakugawa H *et al.* Typing hepatitis B virus by homology in nucleotide sequence: comparison of surface antigen subtypes. *J Gen Virol* 1988; **69:** 2575–83.
11 Lindh M, Andersson AS, Gusdal A. Genotype, nt1858 variants, and geographic origin of hepatitis B virus – Large-scale analysis using a new genotyping method. *J Infect Dis* 1997; **175:** 1285–93.
12 Kao JH, Chen PJ, Lai MY, Chen DS. Hepatitis B genotypes correlate with clinical outcomes in patients with chronic hepatitis B. *Gastroenterology* 2000; **118:** 554–9.
13 Orito E, Ichida T, Sakugawa H *et al.* Geographic distribution of hepatitis B virus (HBV) genotype in patients with chronic HBV infection in Japan. *Hepatology* 2001; **34:** 590–4.
14 Sugauchi F, Orito E, Ohno T *et al.* Spatial and chronological differences in hepatitis B virus genotypes from patients with acute hepatitis B in Japan. *Hepatol Res* 2006; **36:** 107–14.
15 Ozasa A, Tanaka Y, Orito E *et al.* Influence of genotypes and precore mutations on fulminant or chronic outcome of acute hepatitis B virus infection. *Hepatology* 2006; **44:** 326–34.
16 Suzuki Y, Kobayashi M, Ikeda K *et al.* Persistence of acute infection with hepatitis B virus genotype A and treatment in Japan. *J Med Virol* 2005; **76:** 33–9.
17 Tran T, Trinh T, Abe K. New complex recombinant genotype of hepatitis B virus identified in Vietnam. *J Virol* 2008; **82:** 5657–63.
18 Olinger CM, Jutavijittum P, Hübschen JM *et al.* Possible new hepatitis B virus genotype, Southeast Asia. *Emerg Infect Dis* 2008; **14:** 1777–80.
19 Tatematsu K, Tanaka Y, Kurbanov F *et al.* A genetic variant of hepatitis B virus divergent from known human and ape genotype J. *J Virol* 2009; **83:** 10538–47.
20 Usuda S, Okamoto H, Iwanari H *et al.* Serological detection of hepatitis B virus genotypes by ELISA with monoclonal antibodies to type-specific epitopes in the preS2-region product. *J Virol Methods* 1999; **80:** 97–112.
21 Tanaka Y, Sugauchi F, Matsuuraa K *et al.* Evaluation of hepatitis B virus genotyping EIA kit. *Rinsho Byori* 2009; **57:** 42–7.
22 Tadokoro K, Kobayashi M, Yamaguchi T *et al.* Classification of hepatitis B virus genotypes by the PCR-Invader method with genotype-specific probes. *J Virol Methods* 2006; **138:** 30–9.
23 Kimura M. A simple method for estimating evolutionary rates of base substitution through comparative studies of nucleotide sequences. *J Mol Evol* 1980; **16:** 111–20.
24 Takahashi K, Akahane Y, Hino K, Ohta Y, Mishiro S. Hepatitis B virus genomic sequence in the circulation of hepatocellular carcinoma patients: comparative analysis of 40 full-length isolates. *Arch Virol* 1998; **143:** 2313–26.
25 Saitou N, Nei M. The neighbor-joining method: a new method for reconstructing phylogenetic trees. *Mol Biol E* 1987; **4:** 406–25.
26 Norder H, Couroucé AM, Coursaget P *et al.* Genetic diversity of hepatitis B virus strains derived worldwide: genotypes, subgenotypes, and HBsAg subtypes. *Intervirology* 2004; **47:** 289–309.
27 Tanaka Y, Orito E, Yuen MF *et al.* Two subtypes (subgenotypes) of hepatitis B virus genotype C. A novel subtyping assay based on restriction fragment length polymorphism. *Hepatol Res* 2005; **33:** 216–24.
28 Kumar S, Tamura K, Nei M. MEGA3: integrated software for Molecular Evolutionary Genetics Analysis and sequence alignment. *Brief Bioinform* 2004; **5:** 150–63.
29 Matsuura K, Tanaka Y, Hige S *et al.* Distribution of hepatitis B virus genotypes among patients with chronic infection in Japan shifting toward an increase of genotype A. *J Clin Microbiol* 2009; **47:** 1476–83.
30 Kumagai I, Abe K, Oikawa T *et al.* A male patient with severe acute hepatitis who domestically infected with a genotype H hepatitis B virus in Iwate, Japan. *J Gastroenterol* 2007; **42:** 168–75.
31 Koibuchi T, Hitani A, Nakamura T *et al.* Predominance of genotype A HBV in an HBV-HIV-1 dually positive population compared with an HIV-1-negative counterpart in Japan. *J Med Virol* 2001; **64:** 435–40.
32 Tanaka Y, Sanchez LV, Sugiyama M *et al.* Caracteristics of hepatitis B virus genotype G coinfected with genotype H in

chimeric mice carrying human hepatocytes. *Virology* 2008; **376**: 408–15.
33 Sugauchi F, Orito E, Ichida T *et al.* Epidemiologic and virologic characteristics of hepatitis B virus genotype B having the recombination with genotype C. *Gastroenterology* 2003; **124**: 925–32.
34 Owiredu WK, Kramvis A, Kew MC. Hepatitis B virus DNA in serum of healthy black African adults positive for hepatitis B surface antibody alone: possible association with recombination between genotypes A and D. *J Med Virol* 2001; **64**: 441–54.
35 Olinger CM, Venard V, Njayou M *et al.* Phylogenetic analysis of the precore/core gene of hepatitis B virus genotypes E and A in West Africa: new subtypes, mixed infections and recombinations. *J Gen Virol* 2006; **87**: 1163–73.
36 Kurbanov F, Tanaka Y, Fujiwara K *et al.* A new subtype (subgenotype) Ac (A3) of hepatitis B virus and recombination between genotypes A and E in Cameroon. *J Gen Virol* 2005; **86**: 2047–56.
37 Suwannakarn K, Tangkijvanich P, Theamboonlers A, Abe K, Poovorawan Y. A novel recombinant of Hepatitis B virus genotypes G and C isolated from a Thai patient with hepatocellular carcinoma. *J Gen Virol* 2005; **86**: 3027–30.
38 Simmonds P, Midgley S. Recombination in the genesis and evolution of hepatitis B virus genotypes. *J Virol* 2005; **79**: 15467–76.
39 Sitnik R, Pinho JR, Bertolini DA, Bernardini AP, Da Silva LC, Carrilho FJ. Hepatitis B virus genotypes and precore and core mutants in Brazilian patients. *J Clin Microbiol* 2004; **42**: 2455–60.
40 Hino O, Tabata S, Hotta Y. Evidence for increased in vitro recombination with insertion of human hepatitis B virus DNA. *Proc Natl Acad Sci U S A* 1991; **88**: 9248–52.
41 Pineau P, Marchio A, Mattei MG *et al.* Extensive analysis of duplicated-inverted hepatitis B virus integrations in human hepatocellular carcinoma. *J Gen Virol* 1998; **79**: 591–600.

SUPPORTING INFORMATION

ADDITIONAL SUPPORTING INFORMATION may be found in the online version of this article at the publisher's website:

Table S1 Hepatitis B virus DNA-specific oligonucleotide primers used in the study.

SCIENTIFIC REPORTS

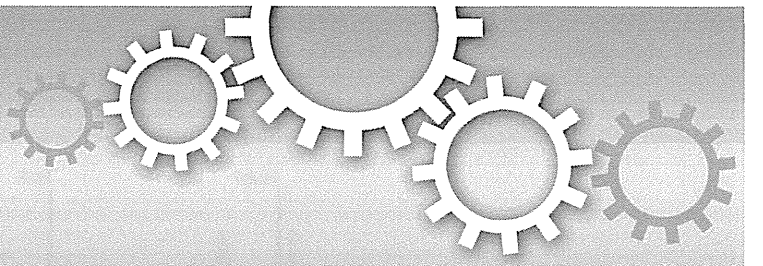

OPEN

SUBJECT AREAS:
TUMOUR IMMUNOLOGY
CANCER PREVENTION
LIVER CANCER
TRANSLATIONAL RESEARCH

Received
2 May 2013

Accepted
4 September 2013

Published
24 September 2013

Correspondence and requests for materials should be addressed to M.O. (otsukamo-tky@umin.ac.jp)

* These authors contributed equally to this work.

Regulation of the expression of the liver cancer susceptibility gene MICA by microRNAs

Takahiro Kishikawa[1]*, Motoyuki Otsuka[1,2]*, Takeshi Yoshikawa[1], Motoko Ohno[1], Akemi Takata[1], Chikako Shibata[1], Yuji Kondo[1], Masao Akanuma[3], Haruhiko Yoshida[1] & Kazuhiko Koike[1]

[1]Department of Gastroenterology, Graduate School of Medicine, The University of Tokyo, Tokyo 113-8655, Japan, [2]Japan Science and Technology Agency, PRESTO, Kawaguchi, Saitama 332-0012, Japan, [3]Division of Gastroenterology, The Institute for Adult Diseases, Asahi Life Foundation, Tokyo 100-0005, Japan.

Hepatocellular carcinoma (HCC) is a threat to public health worldwide. We previously identified the association of a single nucleotide polymorphism (SNP) at the promoter region of the MHC class I polypeptide-related sequence A (MICA) gene with the risk of hepatitis-virus-related HCC. Because this SNP affects MICA expression levels, regulating MICA expression levels may be important in the prevention of HCC. We herein show that the microRNA (miR) 25-93-106b cluster can modulate MICA levels in HCC cells. Overexpression of the miR 25-93-106b cluster significantly suppressed MICA expression. Conversely, silencing of this miR cluster enhanced MICA expression in cells that express substantial amounts of MICA. The changes in MICA expression levels by the miR25-93-106b cluster were biologically significant in an NKG2D-binding assay and an *in vivo* cell-killing model. These data suggest that the modulation of MICA expression levels by miRNAs may be a useful method to regulate HCCs during hepatitis viral infection.

Hepatocellular carcinoma (HCC) is the third most common cause of cancer-related mortality worldwide[1]. Although multiple major risk factors have been identified, such as genetic factors, environmental toxins, alcohol abuse, obesity, and metabolic disorders[2], infection with hepatitis virus B (HBV) or C (HCV) remains the major etiological factor for HCC[1].

Disease progression in HBV-induced or HCV-induced HCC is a multistep phenomenon. The clinical outcomes vary among individuals[1,3,4] because disease progression is influenced by both environmental and genetic risk factors. In terms of genetic susceptibility factors for HCV-induced HCC, we previously identified a single nucleotide polymorphism (SNP) site in the 5′-flanking region of the MICA gene on 6p21.33 (rs2596452) that is strongly associated with progression from chronic hepatitis C to HCC[5]. Individuals with the risk allele A of rs2596452 showed lower serum MICA protein levels[5]. Our subsequent study revealed that the same SNP site was also significantly associated with the risk of HBV-induced HCC[6]. However, interestingly, the risk allele was G in cases of HBV infection, which differed from HCV infection, and the individuals with the risk allele showed increased MICA protein expression levels[6]. Despite the different risk alleles at the same SNP site and inverse association between serum MICA levels and HCC risks in these two etiologies, MICA protein expression levels are significantly associated with susceptibility to HCC in chronic hepatitis viral infection.

MICA is highly expressed on viral-infected and cancer cells and acts as a ligand for NKG2D to activate the antitumor effects of natural killer cells and CD8 T cells[7,8]. This NKG2D-mediated tumor rejection is considered to be effective in the early stages of tumor growth[9–11]. Thus, the expression levels of MICA on the tumor cell surface may determine the antitumor efficacy, and the levels of shedding MICA in serum may act as a decoy of NKG2D to avoid tumor rejection.

Although several stress pathways regulate the transcription of the MICA gene[12,13], cellular microRNAs are suggested to control MICA protein expression via post-transcriptional mechanisms[14,15]. Recently, nucleic-acid-mediated gene therapy has been undergoing clinical trials[16]. Therefore, to target the clinical application of our GWAS results toward prevention of chronic-hepatitis-infection-induced HCC by nucleic-acid-mediated therapy, we determined the regulatory mechanisms of MICA protein expression using miRNA overexpression and miRNA functional silencing.

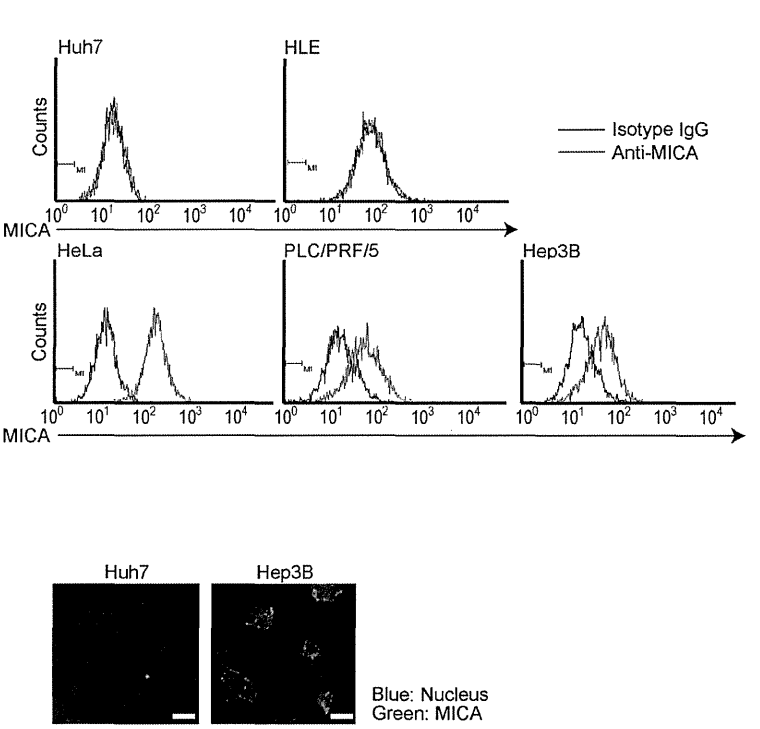

Figure 1 | Expression of MICA protein in HCC cells. (a), Flow cytometry assessment of MICA protein expression in HCC cells (purple lines). Isotype IgG was used for background staining (black lines). HeLa cells were used as the positive control. Representative results from two independent experiments are shown. (b), Immunofluorescence staining for MICA in Huh7 and Hep3B cells. Representative images from two independent experiments are shown. Scale bar, 25 μm.

Results

HCC cell lines differentially express MICA protein. To determine MICA protein levels in HCC cells, four representative HCC cell lines (Huh7, HLE, PLC/PRF/5, and Hep3B cells) underwent flow cytometry to evaluate MICA protein expression because no appropriate antibodies against MICA protein are at present available for western blotting. HeLa cells, which are known to express MICA protein[17], were used as a positive control. Hep3B and PLC/PRF/5 cells expressed substantial MICA protein levels, Huh7 and HLE cells expressed no MICA protein (Figure 1a). This was confirmed by immunocytochemistry using Huh7 and Hep3B cells, which showed staining mainly of cell surfaces (Figure 1b). These results suggest that the MICA protein expression status depends on the cell line examined, even those from the same organ.

The MiR25-93-106b cluster regulates MICA expression. Because upregulation of MICA expression was observed in Dicer-knockdown cells[18], we hypothesized that MICA expression levels may be at least partly regulated by miRNAs. We initially tested miRNAs that might affect MICA expression using reporter constructs into which MICA 3′-untranslated region (3′UTR) sequences were cloned and by transiently overexpressing 76 mature synthetic microRNAs, which were selected on the basis of their hepatic expression level, as in our previous studies[19,20]. Among the microRNAs examined, several may target MICA 3′UTR (Supplementary Figure 1). Among them, we focused on miR93 and miR106b, which were considered to target MICA 3′UTR based partly on the results of our initial miRNA testing described above; in addition, their possible target sequences were identified in the MICA 3′UTR sequences by a computational search using TargetScan 6.0 [21]. Additional reasons that we focused on these two miRNAs were as follows: 1) these miRNAs share the same seed sequences, to which two perfect-match complementary sequences exist in the 3′UTR of MICA (Figure 2a); 2) the target sequences are highly conserved among mammals and are thus likely to be biologically important sites; and 3) these miRNAs are located as a "miR25-93-106b cluster" on human chromosome 7q22.1, and so they may be expressed together under the same transcriptional control. We introduced mutations in the first possible miRNA target sequences of MICA 3′UTR in the reporter constructs (Supplementary Figure 2a); these sequences have a higher likelihood to be target sites, as determined by TargetScan. Co-transfection experiments revealed that reporter activity was suppressed by overexpression of a miR25-93-106b cluster-expressing plasmid (Figure 2b and Supplementary Figure 2b). The overexpression of an unrelated miR (let-7g)-expressing plasmid did not have any significant effects on the reporter activity (Supplementary Figure 2c) and the suppressive effect was lost using constructs with three point mutations in the seed sequences (Figure 2c), suggesting that miR25-93-106b directly targets these sequences and suppresses gene expression.

To confirm these effects, we generated HeLa and Hep3B cell lines that stably expressed the miR25-93-106b-cluster by transducing cells with miR25-93-106b-cluster-expressing lentiviruses (Figure 2d). As expected, the expression of the miR25-93-106b-cluster significantly suppressed MICA protein expression (Figure 2e). However, the expression levels of endogenous miR93 and 106b were not always proportional to the levels of MICA protein expression in the cell lines examined (Supplementary Figure 3). These results suggest that MICA protein expression can be regulated by miR93 and 106b, but that its expression is simultaneously endogenously regulated by other factors (possibly by promoter activities, including epigenetic changes).

Inhibition of miR25-93-106b function increases MICA protein expression. To develop methods of enhancing MICA protein expression levels based on the above results, we examined the

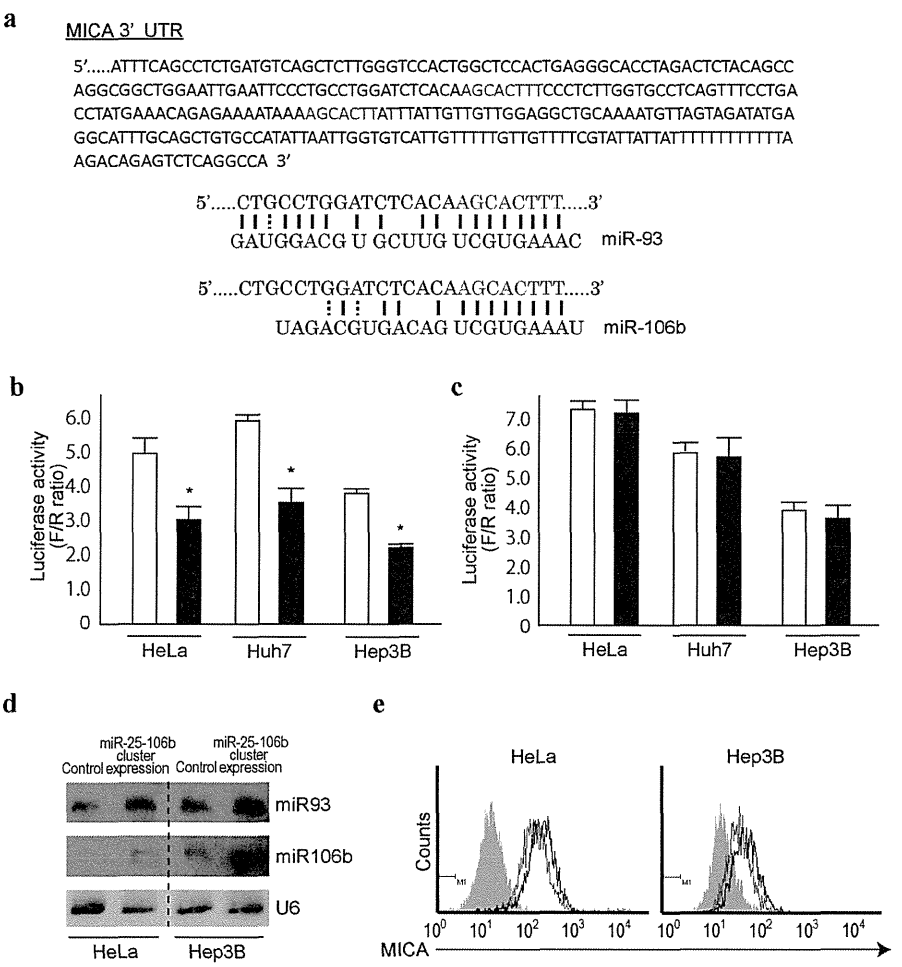

Figure 2 | miR93 and 106b target MICA 3'UTR. (a), Sequences of MICA 3'UTR (upper). Letters in red are the sequences completely matched with the seed regions of miR93 and 106b. The complementarities between the first predicted target in the MICA 3'UTR and miRNA sequences are shown below. (b), (c), Cells were co-transfected with pGL4-TK (renilla luciferase as an internal control), Luc-MICA-3'UTRwt (b) or Luc-MICA-3'UTRmut (c), and either an empty control vector (white bar) or miR25-93-106b-cluster expression plasmid (black bar). Data shows the means ± s.d. of the raw ratios (F/R) obtained by dividing firefly luciferase values with renilla luciferase values of three independent experiments. $*p < 0.05$. (d), miR93 and miR106b expression levels in control and stably miR25-93-106b cluster-expressing cells were determined by northern blotting. U6 levels were used as a loading control. Representative images from two independent experiments are shown. Full-length blot images are available in Supplementary Figure 5. (e), Suppression of MICA expression by overexpression of miRNA93 and 106b. Flow cytometry assessment of MICA protein expression in control (black lines) and stably miR25-93-106b cluster-expressing HeLa and Hep3B cells (red lines). Gray-shaded histograms represent the background staining using isotype IgG. Representative results from two independent experiments are shown.

effects of functional downregulation of miR25-93-106b on MICA expression. We first performed a reporter assay of transient functional silencing of miR25-93-106b using a construct that produces mature anti-sense RNAs designed to silence miR25-93-106b function. As expected, the reporter activities with MICA 3'UTR sequences were enhanced by the functional silencing of miR25-93-106b in HeLa, Hep3B, and Huh7 cells (Figure 3a). However, such effects were not observed using mutant reporter constructs not targeted by those miRNAs (Figure 3b), suggesting that the enhancing effects of the reporter activities were miRNA-dependent.

Next, HeLa, Hep3B, and Huh7 cells were stably transduced with a lentivirus that expresses anti-sense RNAs as described above, and MICA protein expression levels were determined by flow cytometry. Consistent with the reporter assay results, MICA protein expression was increased in HeLa and Hep3B cells by the functional silencing of miR25-93-106b (Figure 3c). However, in Huh7 cells, which express no MICA protein in the normal state, silencing of miR25-93-106b had no effect on MICA protein expression (Figure 3c). These results suggest that MICA protein expression levels can be regulated by modulating miRNA function, albeit only if at least a small quantity of MICA protein is present. In contrast, modulation of miRNA function does not influence MICA protein expression levels when the MICA protein is not expressed, but this could be because there are other forms of regulation at extremely low levels.

MICA protein levels are related to tumor susceptibility to NK cells. To determine the consequences of the modulation of MICA protein expression levels by miRNAs, we first determined the binding ability of NKG2D, a receptor of MICA, using HeLa and Hep3B cells overexpressing the miR25-93-106b cluster or with silencing of miR25-93-106b function. As expected, the levels of NKG2D binding to the cells, theoretically through binding to MICA, were decreased in HeLa and Hep3B cells overexpressing the miR25-93-106b cluster (Figure 4a). On the contrary, the levels of NKG2D binding to the cells were increased in HeLa and Hep3B cells in which miR25-93-106b function had been silenced (Figure 4b).

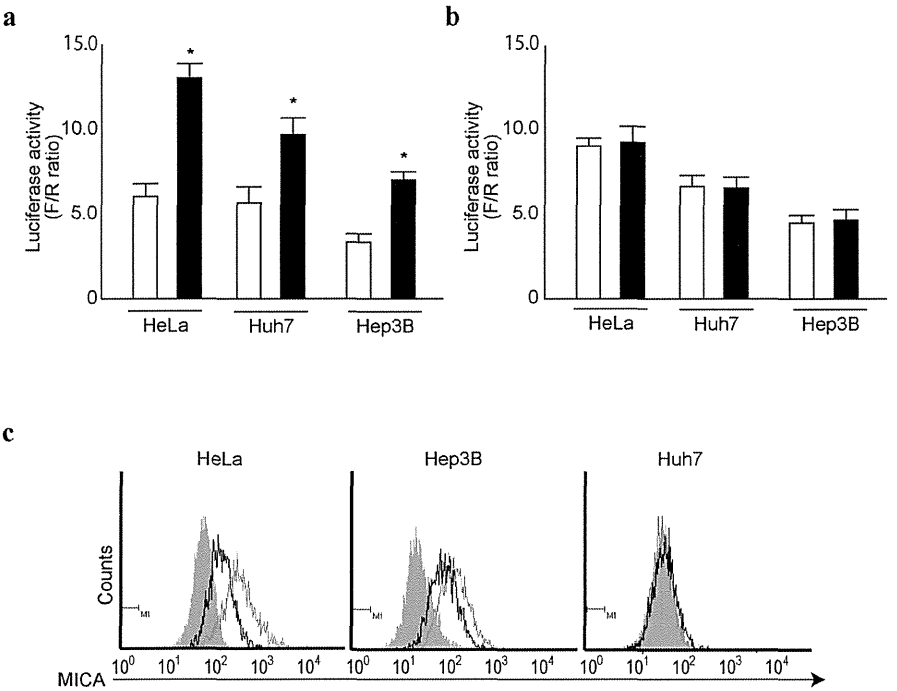

Figure 3 | Silencing of miR25-93-106b cluster enhances MICA expression. (a), (b), Cells were co-transfected with pGL4-TK (internal control), Luc-MICA-3′UTRwt (a) or Luc-MICA-3′UTRmut (b), and either an empty control vector (white bar) or plasmid expressing mature anti-sense sequences of miR25-93-106b cluster (black bar). Data shows the means ± s.d. of the raw ratios (F/R) obtained by dividing firefly luciferase values with renilla luciferase values of three independent experiments. $*p < 0.05$. (c), Enhancement of MICA expression by expression of anti-sense sequences of the miR25-93-106b cluster. Flow cytometry assessment of MICA protein expression in control (black lines) and stably mature anti-sense sequences of miR25-93-106b cluster-expressing cells (green lines). Gray-shaded histograms represent the background staining using isotype IgG. Representative results from three independent experiments are shown.

Next, to determine whether tumor cells with different miRNA-induced MICA protein expression levels exhibited differing susceptibilities to NK-cell-mediated killing *in vivo*, we performed a tumor-clearance assay that measures short-term *in vivo* killing by NK cells[22]. Hep3B control cells, Hep3B cells with miR25-93-106b cluster overexpression, or Hep3B cells with miR25-93-106b and HA-tagged MICA overexpression, labeled with fluorescent DiO, were injected into C57Black6/J mouse tail veins together with an equal number of HeLa cells labeled with Dil (internal reference control). After 5 h, surviving Hep3B and HeLa cells in the lungs were enumerated by flow cytometry. The number of Hep3B cells that had survived divided by the number of HeLa cells that had survived represents the relative killing of Hep3B cells *in vivo*. As shown by the *in vitro* binding assay using NKG2D, the killing rate of Hep3B cells in which miRNA function had been silenced was higher, and that of cells overexpressing miRNAs was lower, than that of control cells. The effects of miRNA overexpression were similar to those obtained in MICA knocked-down Hep3B cells (supplementary Figure 4). Additionally, the lower cell-killing rate in Hep3B cells overexpressing miRNA was antagonized by the co-expression of exogenous MICA protein (Figure 4c), suggesting that the decreased clearance was mediated by reduced MICA expression levels secondary to overexpression of miRNAs. These results suggest that tumor progression and invasion can be regulated by expression or silencing of miRNAs in at least some cells by regulation of MICA expression levels.

Discussion

In this study, we showed that the miR25-93-106b cluster modulates MICA protein expression by HCC cells. Because our previous GWAS analyses identified that MICA is the critical gene determining HCC susceptibility in patients with chronic hepatitis infection[5,6], the herein-described methods of modulating MICA expression may be useful for developing novel methods of prevention and therapeutics against HCCs.

MICA is a membrane protein that acts as a ligand for NKG2D to activate innate anti-tumor effects through natural killer and $CD8^+$ cells[7]. Our previous GWAS study showed that a risk allele at the SNP in the MICA promoter region was significantly associated with the susceptibility of HCV-induced HCC as well as with lower serum MICA levels. Although polymorphisms at the same SNP site were also associated with HBV-induced HCC, the risk allele determining the susceptibility of HCC was somehow different from that in HCV-induced HCC. While the reason why different MICA gene variations act as risk alleles at the same SNP site between HBV- and HCV-induced HCC has not been elucidated, it is assumed that changes in the membrane-bound MICA and soluble MICA levels due to differences in post-translational processing according to virus type may affect the risk allele results. In any case, because the importance of the regulation of MICA expression levels to prevent development of HCC due to chronic hepatitis viral infection cannot be denied, the regulation of MICA levels by microRNAs as shown here may be useful for the development of preventive methods of preventing HCC development during chronic hepatitis infection.

While several cellular signaling pathways lead to upregulation of MICA[12,13], we used microRNAs to regulate the expression levels of MICA in this study. As shown by the results of our GWAS analyses, which found that the polymorphisms in the promoter region of MICA are associated with changes in the sMICA levels[5,6], promoter activities of the MICA gene also have significant effects on MICA expression levels[23]. Our results showed that miR93 and 106b expression levels were not always correlated with those of MICA in HCC cell lines, suggesting that the regulation of MICA expression is not solely

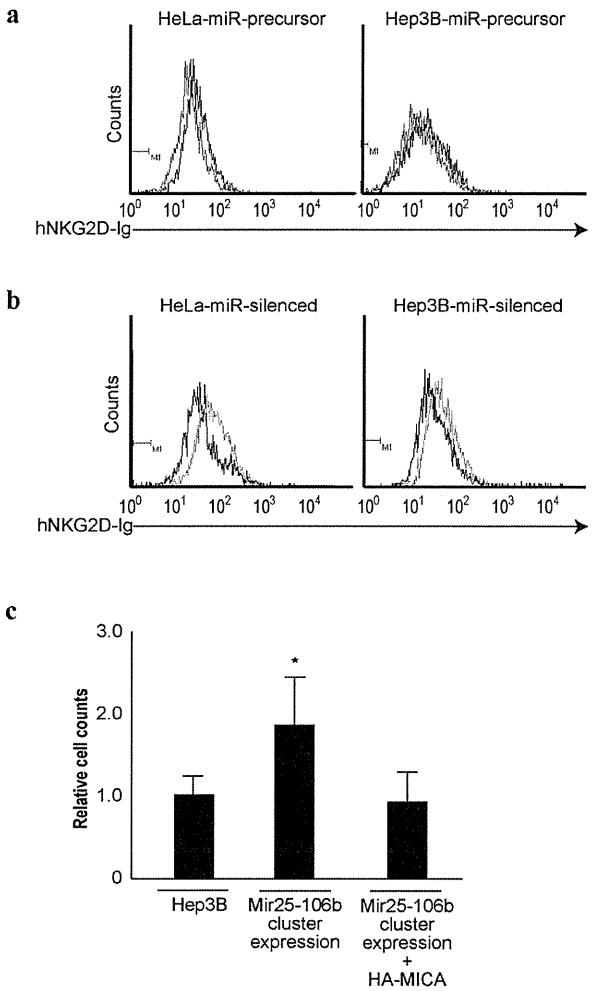

Figure 4 | NKG2D binding levels change in proportion to MICA expression levels. (a), (b), Flow cytometry of human IgG-fused NKG2D binding to the control (black lines), miR25-93-106b cluster-expressing cells (red lines) (a), and mature anti-sense sequences of miR25-93-106b cluster-expressing cells (green lines) (b). Representative results from three independent experiments are shown. (c), *In vivo* killing of DiO-labeled Hep3B and Dil-labeled HeLa cells (internal control cells) injected together into the tail veins of six mice in each group. Fluorescence intensities were quantified by flow cytometry as the ratio of Hep3B to HeLa cells in the lungs. The data from control Hep3B cells were set as 1.0. Data represent the means ± s.d. of three independent experiments. $*p < 0.05$.

dependent on miRNAs. In addition, in cells with no endogenous MICA expression, such as Huh7 cells, modulation of microRNA expression had no effect on the regulation of MICA expression. This suggests that at least low-level endogenous expression, which may be determined by promoter activities, are needed for regulation by miRNA. Therefore, changes in promoter activities and epigenetic changes in the MICA gene should also be determined. This will facilitate application of the regulatory function of miRNAs reported here.

One class of antisense oligonucleotides, namely locked nucleic acids, can be used to sequester microRNAs in the liver of various animals, including humans[16,24,25]. A clinical trial targeting miR-122 with the anti-miR-122 oligonucleotides miravirsen, the first miRNA-targeted drug, is underway for the treatment of HCV infection[16]. Thus, nucleic-acid-mediated gene therapy is becoming a realistic option. Modulation of MICA expression levels by such nucleic-acid-mediated therapy based on the results presented herein may also be a promising option for prevention and/or therapy of HCC.

In summary, we have shown that the miR25-93-106b cluster can be used to modulate MICA expression levels in HCC cells. Based on our GWAS results and associated studies, regulation of MICA protein expression levels is crucial to prevent the development of HCC during chronic hepatitis viral infection. It is important to identify the other factors that regulate MICA transcriptional activities as well as the post-translational processes and their association with susceptibility to HCCs. That said, miRNA regulation of MICA expression as shown here may facilitate regulation of the host innate immune system in an HCC-suppressive manner during chronic hepatitis viral infection.

Methods

Cell culture. The human HCC cell lines Huh7, HLE, PLC/PRF/5, and Hep3B were obtained from the Japanese Collection of Research Bioresources (JCRB, Osaka, Japan). The human cervical cancer cell line HeLa was obtained from the American Type Culture Collection (ATCC, Rockville, MD). All cells were maintained in Dulbecco's modified Eagle's medium supplemented with 10% fetal bovine serum.

Mouse. Experimental protocols were approved by the Ethics Committee for Animal Experimentation at the Graduate School of Medicine, the University of Tokyo and the Institute for Adult Disease, Asahi Life Foundation, Japan and conducted in accordance with the Guidelines for the Care and Use of Laboratory Animals of the Department of Medicine, the University of Tokyo, and the Institute for Adult Disease, Asahi Life Foundation.

Flow cytometry. Cells were hybridized with anti-MICA (1 : 500; R&D Systems, Minneapolis, MN) and isotype control IgG (1 : 500; R&D Systems) in 5% BSA/1% sodium azide/PBS for 1 h at 4°C. After washing, cells were incubated with goat anti-mouse Alexa 488 (1 : 1000; Molecular Probes, Eugene, OR) for 30 min. Flow cytometry was performed and data analyzed using Guava Easy Cyte Plus (GE Healthcare, Little Chalfont, UK).

Reporter plasmid construction, transient transfections, and luciferase assays. The reporter plasmid for the analysis of the effects of miRNAs on MICA 3′UTR were constructed by subcloning the MICA 3′UTR sequences from pLightSwitch-MICA 3UTR (SwitchGear Genomics, Menlo Park, CA) into the pGL4.50 vector (Promega, Madison, WI) at the *FseI* site by the In-Fusion method (Clontech, Mountain View, CA) to insert the MICA 3′UTR sequences into the 3′-UTR of the firefly luciferase gene, which was under the control of the CMV promoter. The sequences of the primers were 5′-CTA GAG TCG GGG CGG CG GCC ATT TCA GCC TCT GAT GTC AGC-3′ and 5′-GTC TGC TCG AAG CGG CCG GCC TGG CCT GAG ACT CTG TCT TAA-3′. The resultant plasmid (Luc-MICA 3′UTRwt) was used as a template for the construction of mutant reporter plasmid (Luc-MICA 3′UTRmut), which carries three point mutations in the seed sequences of miR93 and 106b in the MICA 3′UTR, itself generated by a Quik Change II XL Site-directed Mutagenesis Kit (Stratagene, Heidelberg, Germany) according to the manufacturer's instructions. Transient transfection and reporter assays were performed as described previously[26].

Lentiviral constructs, viral production, and transduction. To generate a neomycin-resistant miR25-93-106b cluster-expressing lentiviral construct, copGFP in the pmiRNA25-93-106b cluster-expressing plasmid (System Biosciences, Mountain View, CA) was replaced with a neomycin resistant gene, which was subcloned from the pCDH-Neo vector (System Biosciences), at the *FseI* site. The primers used were 5′-GCT ACC GCT ACG AGG CCG GCC CAT GAT TGA ACA AGA TGG ATT GCA-3′ and 5′-TCG CCG ATC ACG CGG CCG GCC TCA GAA GAA CTC GTC AAG AAG GC-3′. To remove the copGFP region from pmiRZIP25-93-106b (System Biosciences), a construct expressing mature anti-sense sequences of the miR25-93-106b cluster, sequences coding the GFP gene were removed by excision with *XbaI* and *PstI* sites followed by connecting the cut ends with annealed oligonucleotides (5′-CTA GAC GCC ACC ATG CTG CA-3′ and 5′-GCA TGG TGG CGT-3′) to maintain the coding frame and the expression of the downstream puromycin-resistance gene. To generate HA-tagged MICA protein overexpressing the lentiviral construct, MICA cDNA was amplified by PCR using a Halo-tag-MICA–expressing plasmid (Promega, Madison, WI) as a template and cloned into a pCDH-puro vector (System Biosciences) at the *NotI* site. The primer sequences used were 5′-ATC GGA TCC GCG GCC GCA CCA TGT ACC CAT ACG ATG TTC CAG ATT ACG CTA TGG GGC TGG GCC CGG TC-3′ and 5′-AGA TCC TTC GCG GCC GCT TAG GCG CCC TCA GTG GAG C-3′. Let-7g precursor expressing plasmid was generated by inserting about 1,000 bp long PCR product around the let-7g genomic region into pCDH-puro vector using *Xba*1 and *Not*1 sites. The production and concentration of lentiviral particles were described previously[27]. shRNA against MICA-producing lentiviral particles with puromycin resistant gene were purchased from SantaCruz Biotechnology (sc-4924-V, Dallas, TX). Cells were transduced with lentiviruses using

polybrene (EMD Millipore, Billerica, MA). The selections were performed with 400 μg/mL G418 and 2 μg/mL (HeLa) or 6 μg/mL (Hep3B) puromycin.

Immunocytochemistry. Cells on two-well chamber slides were fixed with 4% paraformaldehyde. Fixed cells were probed with the primary MICA antibody (R&D Systems) for 1 h after blocking with 5% normal goat serum for 30 min. Cells probed with the MICA antibody were incubated with the secondary Alexa Fluor 488 goat anti-mouse antibody (Molecular Probes) for 30 min. Slides were mounted using VectaShield with DAPI (Vector Labs, Burlingame, CA).

Northern blotting of miRNAs. Northern blotting of miRNAs was performed as described previously[27]. Briefly, total RNA was extracted using TRIzol Reagent (Invitrogen, Carlsbad, CA) according to the manufacturer's instructions. Ten micrograms of RNA were resolved in denaturing 15% polyacrylamide gels containing 7 M urea in 1 × TBE and then transferred to a Hybond N+ membrane (GE Healthcare) in 0.25 × TBE. Membranes were UV-crosslinked and prehybridized in hybridization buffer. Hybridization was performed overnight at 42°C in ULTRAhyb-Oligo Buffer (Ambion) containing a biotinylated probe specific for miR93 (cta cct gca cga aca gca ctt tg) and 106b (atc tgc act gtc agc act tta), which had previously been heated to 95°C for 2 min. Membranes were washed at 42°C in 2 × SSC containing 0.1% SDS, and the bound probe was visualized using a BrightStar BioDetect Kit (Ambion). Blots were stripped by boiling in a solution containing 0.1% SDS and 5 mM EDTA for 10 min prior to rehybridization with a U6 probe (cac gaa ttt gcg tgt cat cct t).

miRNA library screening. To screen for miRNAs that target MICA 3′-UTR, synthetic miRNA mimics and reporter constructs were used as described previously[19,20]. Seventy-six types of synthetic mature miRNAs that are highly expressed in the liver[28] were custom-made (B-Bridge, Tokyo, Japan) and transfected by RNAi Max (Life Technologies, Carlsbad, CA) into Huh7 cells in 96-well plates that had been transfected 24 h before with Luc-MICA 3′UTRwt. The cells were then incubated for another 24 h. As negative controls, oligonucleotides of artificial sequences were applied[19]. The luciferase activities were measured using a GloMax 96 Microplate Luminometer (Promega). The experiments were performed in duplicate.

NKG2D binding assay. Cells were incubated with 4 μg of recombinant human NKG2D fused to human IgG1 Fc chimera protein. After washing, cells were incubated with an Alexa488-conjugated affinity purified F(ab')2 fragment of goat anti-human IgG (Jackson ImmunoResearch Laboratories, West Grove, PA). As a negative control, cells were incubated with only Alexa488 anti-human IgG. The intensity of the fluorescence was determined by flow cytometry.

***In vivo* cell-killing assay.** Hep3B cells and HeLa cells were labeled with the fluorescent dye VybrantDiO and DiI (Molecular Probes), respectively. Cells were mixed at a density of 2×10^7 in 1-ml PBS, and 200 μl was injected into the tail vein. Five hours later, lungs were collected, and single-cell suspensions were collected using a cell strainer. Fluorescence was assayed by flow cytometry, and the ratio of the experimental Hep3B cells to HeLa cells (internal control) was calculated.

Statistical analysis. Statistically significant differences between groups were determined using Student's *t*-test when variances were equal. When variances were unequal, Welch's *t*-test was used instead. *P*-values of < 0.05 were considered to indicate statistical significance.

1. El-Serag, H. B. Epidemiology of viral hepatitis and hepatocellular carcinoma. *Gastroenterology* **142**, 1264–1273 (2012).
2. Sherman, M. Hepatocellular carcinoma: New and emerging risks. *Dig Liver Dis* **42**, S215–222 (2010).
3. Arzumanyan, A., Reis, H. M. & Feitelson, M. A. Pathogenic mechanisms in HBV- and HCV-associated hepatocellular carcinoma. *Nat Rev Cancer* **13**, 123–135 (2013).
4. Urabe, Y. *et al.* A genome-wide association study of HCV-induced liver cirrhosis in the Japanese population identifies novel susceptibility loci at the MHC region. *J Hepatol* (2013).
5. Kumar, V. *et al.* Genome-wide association study identifies a susceptibility locus for HCV-induced hepatocellular carcinoma. *Nat Genet* **43**, 455–458 (2011).
6. Kumar, V. *et al.* Soluble MICA and a MICA variation as possible prognostic biomarkers for HBV-induced hepatocellular carcinoma. *PLoS One* **7**, e44743 (2012).
7. Maccalli, C., Scaramuzza, S. & Parmiani, G. TNK cells (NKG2D+ CD8+ or CD4+ T lymphocytes) in the control of human tumors. *Cancer Immunol Immunother* **58**, 801–808 (2009).
8. Jinushi, M. *et al.* Impairment of natural killer cell and dendritic cell functions by the soluble form of MHC class I-related chain A in advanced human hepatocellular carcinomas. *J Hepatol* **43**, 1013–1020 (2005).
9. Diefenbach, A., Jensen, E. R., Jamieson, A. M. & Raulet, D. H. Rae1 and H60 ligands of the NKG2D receptor stimulate tumour immunity. *Nature* **413**, 165–171 (2001).
10. Hayakawa, Y. Targeting NKG2D in tumor surveillance. *Expert Opin Ther Targets* **16**, 587–599 (2012).
11. Guerra, N. *et al.* NKG2D-deficient mice are defective in tumor surveillance in models of spontaneous malignancy. *Immunity* **28**, 571–580 (2008).
12. Bauer, S. *et al.* Activation of NK cells and T cells by NKG2D, a receptor for stress-inducible MICA. *Science* **285**, 727–729 (1999).
13. Eleme, K. *et al.* Cell surface organization of stress-inducible proteins ULBP and MICA that stimulate human NK cells and T cells via NKG2D. *J Exp Med* **199**, 1005–1010 (2004).
14. Yadav, D., Ngolab, J., Lim, R. S., Krishnamurthy, S. & Bui, J. D. Cutting edge: down-regulation of MHC class I-related chain A on tumor cells by IFN-gamma-induced microRNA. *J Immunol* **182**, 39–43 (2009).
15. Stern-Ginossar, N. & Mandelboim, O. An integrated view of the regulation of NKG2D ligands. *Immunology* **128**, 1–6 (2009).
16. Janssen, H. L. *et al.* Treatment of HCV Infection by Targeting MicroRNA. *N Engl J Med* **368**, 1685–94 (2013).
17. Salih, H. R., Rammensee, H. G. & Steinle, A. Cutting edge: down-regulation of MICA on human tumors by proteolytic shedding. *J Immunol* **169**, 4098–4102 (2002).
18. Tang, K. F. *et al.* Decreased Dicer expression elicits DNA damage and up-regulation of MICA and MICB. *J Cell Biol* **182**, 233–239 (2008).
19. Takata, A. *et al.* MicroRNA-22 and microRNA-140 suppress NF-κB activity by regulating the expression of NF-κB coactivators. *Biochem Biophys Res Commun* **411**, 826–831 (2011).
20. Yoshikawa, T. *et al.* Silencing of microRNA-122 enhances interferon-a signaling in the liver through regulating SOCS3 promoter methylation. *Sci. Rep.* **2**, 637 (2012).
21. Lewis, B. P., Burge, C. B. & Bartel, D. P. Conserved seed pairing, often flanked by adenosines, indicates that thousands of human genes are microRNA targets. *Cell* **120**, 15–20 (2005).
22. Gazit, R. *et al.* Lethal influenza infection in the absence of the natural killer cell receptor gene Ncr1. *Nat Immunol* **7**, 517–523 (2006).
23. Lo, P. H. *et al.* Identification of a Functional Variant in the MICA Promoter Which Regulates MICA Expression and Increases HCV-Related Hepatocellular Carcinoma Risk. *PLoS One* **8**, e61279 (2013).
24. Lanford, R. E. *et al.* Therapeutic silencing of microRNA-122 in primates with chronic hepatitis C virus infection. *Science* **327**, 198–201 (2010).
25. Elmén, J. *et al.* LNA-mediated microRNA silencing in non-human primates. *Nature* **452**, 896–899 (2008).
26. Kojima, K. *et al.* MicroRNA122 is a key regulator of α-fetoprotein expression and influences the aggressiveness of hepatocellular carcinoma. *Nat Commun* **2**, 338 (2011).
27. Takata, A. *et al.* MicroRNA-140 acts as a liver tumor suppressor by controlling NF-κB activity by directly targeting DNA methyltransferase 1 (Dnmt1) expression. *Hepatology* **57**, 162–170 (2013).
28. Krützfeldt, J. *et al.* Silencing of microRNAs in vivo with 'antagomirs'. *Nature* **438**, 685–689 (2005).

Acknowledgments

This work was supported by Grants-in-Aid from the Ministry of Education, Culture, Sports, Science and Technology, Japan (#25293076, #25460979, and #24390183) (to M.Otsuka, Y.K. and K.K.), by Health Sciences Research Grants of The Ministry of Health, Labour and Welfare of Japan (to K.K.), and by grants from the Okinaka Memorial Institute for Medical Research, the Liver Forum in Kyoto, and the Princess Takamatsu Cancer Research Fund (to M.Otsuka).

Author contributions

T.K., M. Otsuka and K.K. planned the research and wrote the paper. T.K., M. Otsuka, T.Y., M. Ohno, A.T., C.S. and Y.K. performed the majority of the experiments. M.A. and H.Y. supported several experiments and analyzed the data. K.K. supervised the entire project.

Additional information

Supplementary information accompanies this paper at http://www.nature.com/scientificreports

Competing financial interests: The authors declare no competing financial interests.

How to cite this article: Kishikawa, T. *et al.* Regulation of the expression of the liver cancer susceptibility gene MICA by microRNAs. *Sci. Rep.* **3**, 2739; DOI:10.1038/srep02739 (2013).

EXPERIMENTAL CELL RESEARCH 319 (2013) 113–121

Available online at www.sciencedirect.com

SciVerse ScienceDirect

journal homepage: www.elsevier.com/locate/yexcr

Research Article

Leucine-rich repeat-containing G protein-coupled receptor 5 regulates epithelial cell phenotype and survival of hepatocellular carcinoma cells

Mariko Fukuma[a], *Keiji Tanese*[b], *Kathryn Effendi*[a], *Ken Yamazaki*[a], *Yohei Masugi*[a], *Mariko Suda*[a], *Michiie Sakamoto*[a,*]

[a]*Department of pathology, Keio University School of Medicine, Shinjuku-ku, Tokyo 160-8582, Japan*
[b]*Department of dermatology, Keio University School of Medicine, Shinjuku-ku, Tokyo 160–8582, Japan*

ARTICLE INFORMATION

Article Chronology:
Received 28 June 2012
Received in revised form
11 October 2012
Accepted 26 October 2012
Available online 2 November 2012

Keywords:
LGR5
GPR49
Hepatocellular carcinoma
Morphology
Motility

ABSTRACT

The leucine-rich repeat containing G protein-coupled receptor 5 (LGR5), also known as GPR49, is a seven-transmembrane receptor that is expressed in stem cells of the intestinal crypts and hair follicles of mice. LGR5 is overexpressed in some types of human cancer, and is one of the target genes of the Wnt signaling pathway. To explore the function of LGR5 in cancer cells, stable hepatocellular carcinoma (HCC) cell lines expressing FLAG-tagged LGR5 were established. Overexpression of LGR5 resulted in changes in cell shape from an extended flat (mesenchymal) phenotype to a round aggregated (stem cell-like) phenotype. Cells transfected with LGR5 showed higher colony forming activity, and were more resistant to a cytotoxic drug than cells transfected with empty vector. Overexpression of LGR5 inhibited cell motility. LGR5-transfected cells formed nodule type tumors in the livers of immunodeficient mice, whereas empty vector-transfected cells formed more invasive tumors. Down-regulation of LGR5 changed the morphology of HCC cells from the aggregated phenotype to an extended spindle phenotype, and cell motility was increased. This is the first study reporting the functional role of LGR5 in the biology of HCC cells, and the results suggest that aberrant expression of LGR5 regulates epithelial cell phenotype and survival.

Introduction

The leucine-rich repeat-containing G protein-coupled receptor 5 (LGR5), aliases G protein-coupled receptor 49 (GPR49), FEX, GPR67, GRP49, HG38, MGC117008, is structurally related to members of the glycoprotein hormone receptor family. In mice, deficiency of this gene causes neonatal lethality as a result of ankyloglossia [1]. LGR5 deficiency also induces premature differentiation of Paneth cells [2]. Recent studies from the Netherlands showed that in a mouse model, the homolog of this gene was a marker of intestinal and hair follicle stem cells. Introduction of an adenomatous polyposis coli (APC) mutation into LGR5-expressing cells increased the incidence of adenomas in mouse intestinal epithelial cells [3–5].

*Correspondence to: Department of pathology, Keio University School of Medicine, 35 Shinanomachi, Shinjuku-ku, Tokyo 160-8582, Japan. Fax: +81 3 3353 3290.
E-mail address: msakamot@z5.keio.jp (M. Sakamoto).

0014-4827/$ - see front matter © 2012 Elsevier Inc. All rights reserved.
http://dx.doi.org/10.1016/j.yexcr.2012.10.011

LGR5 has been reported to be upregulated in several tumors. We have previously shown that expression of LGR5 in the noncancerous liver was very low, however LGR5 is frequently overexpressed in hepatocellular carcinoma (HCC) with β-catenin mutations [6]. Although mutations of β-catenin are found in nearly 40% of HCC, the LGR5 has not been reported as the marker of hepatocyte, nor mentioned as a marker gene for liver regeneration. LGR5 also has been identified as a gene responsible to promote cell proliferation and tumor formation in basal cell carcinoma (BCC), a common malignant tumor of the skin [7]. High levels of LGR5 expression were also reported in colon and ovarian carcinomas [8], and we have shown that a high level of LGR5 expression in colorectal cancer was significantly correlated with tumor stage [9]. One study using colorectal cancer cell lines showed that suppression of LGR5 expression enhances tumorigenesis and is linked to a more mesenchymal phenotype [10].

There are some evidences suggest that LGR5 is a downstream target gene of Wnt signaling pathway [2,6,11,12]. The Wnt signaling pathway comprises a vast number of protein interactions and plays a critical role in morphogenesis and tumorigenesis. To date, three main pathways related to Wnt signaling have been identified: the β-catenin-dependent, planar cell polarity, and Wnt/Ca^{2+} pathways [13]. The β-catenin-dependent pathway, otherwise known as the canonical pathway, has been the most intensively studied. Mutations or deletions in AXN1/2 or APC genes inhibit the phosphorylating activity of GSK-3β, thereby stabilizing cytoplasmic β-catenin, and provoking aberrant cellular gene expression. Mutations at sites that affect β-catenin phosphorylation also cause cytoplasmic accumulation of β-catenin and lead to dysregulation of the pathway. Recently, LGR5 was reported to be a receptor of R-spondins which were known to be a potent family protein mediating Wnt/β-catenin and Wnt/PCP signaling [11,12,14]. Acquirement of stem cell-like properties in various tumors have greatly increased the possible role of these cells in tumorigenesis [15,16]. Upregulation of LGR5 in several tumors with increased Wnt signaling pathway suggests the possible role of LGR5 gene in oncogenesis and morphogenesis [6–9]. However, the functional role of LGR5 in tumor cells is still poorly understood. In this study, we aimed to analyze the function of LGR5 in hepatocellular carcinoma cells.

Materials and methods

Cell culture and chemicals

Cells were cultured in RPMI 1640 supplemented with 10% fetal bovine serum, 100 U/ml of penicillin and 100 μg/ml of streptomycin [6,9]. HepG2 containing a deletion of exon 3 of the β-catenin gene and PLC/PRF/5 containing a deletion of exon 4 of the AXIN1 were used as cell lines with activated Wnt signaling and high levels of LGR5 mRNA[17]. KYN2 cells were used as a cell line with low expression of LGR5 mRNA [6,9].

Plasmids, transfection, and establishment of stable transfectants

A FLAG-tagged LGR5 expression vector (LGR5-FL) was constructed by inserting the full-length coding cDNA for human LGR5 (RZPD, Berlin, Germany) into the Bgl II site of p3XFLAG-CMV-14 (Sigma-Aldrich, St. Louis, MO, USA). KYN-2 cells were transfected with LGR5-FL or empty vector using Lipofectamine LTX reagent (Invitrogen, Carlsbad, CA, USA). Production of LGR5-FL protein was detected by confocal laser scanning microscopy (LSM510, Carl Zeiss, Germany) and western blot analysis, using the FLAG M2 antibody (Sigma-Aldrich). F-actin was stained with TexasRed X-phalloidin (Molecular Probes, Eugene, OR, USA) and nucleus was stained with VECTASHIELD Mounting Medium with DAPI (Vector Laboratories Inc. Burlingame, CA, USA). Anti-E-cadherin (ALX-804-201-C100, Enzo Life Sciences, Inc.) and anti-β-catenin (E-5, Santa Cruz Biotechnology, Inc.) antibodies were used for immunofluorescent staining. Colonies that formed in 0.3% soft agar medium containing G418 (Invitrogen) were picked and propagated. Each colony was purified by three sequential series of limiting dilutions. Ultimately, six LGR5-transfected clones (KY-B1, KY-G1, KY-G2, KY-G6, KY-F3, and KY-S1) and five empty vector-transfected clones (KY-V2, KY-V3, KY-V4, KY-V5, and KY-V6) were established. Protein levels were analyzed by western blotting and mRNA levels were analyzed by quantitative PCR. Canonical Wnt signaling activity was measured with the TCF-luciferase reporter system (TOPflash/FOPflash, Upstate Millipore Co.), and the results are shown as the ratio of TOPflash to FOPflash (TOP/FOP).

Quantitative polymerase chain reaction (qPCR)

Total RNA was isolated from cells using the RNeasy Mini Kit, including DNase treatment (Qiagen KK, Tokyo, Japan). cDNA was synthesized using the PrimeScript® RT reagent kit (Perfect Real Time; Takara Bio, Shiga, Japan), and qPCR was performed on a Thermal Cycler Dice Real Time System using SYBR *Premix Ex Taq*™ (Perfect Real Time; Takara Bio). The primer sequences for qPCR were as follows: GAPDH forward, 5′–ATCATCCCTGCCTCTACTGG-3′; GAPDH reverse, 5′–TTTCTAGACGGCAGGTCAGGT-3′; LGR5 forward, 5′–GAGGATCTGGTGAGCCTGAGAA-3′; LGR5 reverse, 5′–CATAAGTGATGCTGGAGCTGGTAA-3′; RSPO1 forward, 5′–AAGGCTGTGAGCTCTGCTCT-3′; RSPO1 reverse, 5′–ATGTCGTTCCTCTCCAGCAG3′. GAPDH was used as a reference. Fold induction values were calculated using the $2^{-\Delta\Delta\ Ct}$ method. All experiments were performed in triplicate and repeated at least three times in separate experiments; representative data are shown.

Cell proliferation, cell migration, and cytotoxicity assays

Cells were plated in 24-well dishes, and the number of cells was counted in a hemocytometer after staining with trypan blue. Ratio number of cells represents the total mean number of LGR5-overexpressing cells or empty vector cells for each day compared to the total mean number of cells at day 0. RNA interference experiments were performed using siRNA. The target sequences were as follows: LGR5-585, 5′–GAA CAA AAU ACA CCA CAUA-3′; LGR5-662, 5′–GAA UCC ACU CCC UGG GAAA-3′. AllStars Negative Control siRNA (Qiagen) was used as a control. Cells were transfected with the final concentration of 10 nM siRNA using Lipofectamine RNAiMAX transfection reagent (Invitrogen).

For cytotoxicity tests, cells were treated with puromycin for 20 h, washed with PBS and covered with growth medium containing 0.3% agar. Cells were cultured for 2 weeks with occasional replenishment of the medium. Colonies were stained

with nitro blue tetrazolium reagent and photographed for counting. For cell migration assays, cells were placed in six-well dishes and incubated for two days. The confluent monolayer cultures were scratched and photographed after 24 h. The width of each scratch was measured at ten points and more than five scratches were measured for each group. For RNA interference assays, cells were transfected with siRNAs for 20 h and replated in six-well dishes. The monolayer cultures that formed 24 h later were scratched and photographed as described previously.

Tumor formation assays

Clones containing LGR5-FL or empty vector were transplanted into the subcapsular region of the livers of NOG mice (NOD/Shi-scid/IL-2γ−/−) at 5×10^6 cells per mouse. The tumors that formed in the liver were resected, fixed with 10% neutral-formalin, and used for histological analysis. For metastasis assays, cells were inoculated into the subcapsular region of the spleens of NOG mice, and tumors that formed in the liver were used for histological analysis.

Statistical analysis

Differences were assessed for statistical significance using Student's *t*-test, with the level of significance being $P<0.05$.

Results

Establishment of LGR5-overexpressing clones

To determine the function of LGR5 in cancer cells, stable clones containing the LGR5 gene were established. We have tested several commercially available anti-LGR5 antibodies, however, we could not obtain good results in order to detect LGR5 protein expression in HCC tissue. Thus, we constructed a FLAG-tagged LGR5-expression vector (LGR5-FL), and production of the protein was detected by immunofluorescence microscopy and western blot analysis using anti-FLAG antibody. When LGR5-FL was transfected into KYN-2 cells, the protein was localized mostly in the cytoplasm and cytoplasmic membrane (Fig. 1A). To establish stable clones, LGR5-FL or empty vector was transfected into KYN-2 cells, and G418-resistant colonies that formed in soft agar medium were purified by three series of limiting-dilution propagations. Six clones stably transfected with LGR5-FL (KY-B1, KY-G1, KY-G2, KY-G6, KY-F3, KY-S1) and five clones stably transfected with empty vector (KY-V2, KY-V3, KY-V4, KY-V5, KY-V6) were isolated. The LGR5 protein (~100 kD) was detected by western bot analysis (Fig. 1B), and mRNA levels were measured by qPCR (Fig. 1C). The KY-G1 and KY-S1 transfectants expressed high levels of LGR5 protein and mRNA. The protein and mRNA levels in each of the clones were well correlated, and the same levels were maintained after several passages. Only the results for three vector-transfectants are shown in Fig. 1B and C, but the other clones showed similar results.

Phase contrast microscopy showed that LGR5-overexpressing KY-G1 and KY-S1 cells had a round shape and aggregated together, whereas KY-V2 and KY-V3 cells had a flat extended shape and spread on the culture dishes (Fig. 1D). LGR5-transfectants stacked up on the surface of the culture dishes, whereas empty vector–transfectants formed flat monolayers (Fig. 1E). Phalloidin staining showed strong F-actin signals between KY-G1 cells (so-called cortical actin), whereas KY-V2 cells showed a flat extended shape with F-actin in the cytoplasm (Fig. 1F). Distinct fluorescent signals of E-cadherin were located between KY-G1 cells (Fig. 1G). Similar distribution of β-catenin was also seen in KY-G1 and KY-V2 cells, respectively (Fig. 1H). Accumulation of β-catenin in nuclei which is often seen in cell with activated Wnt signaling could not be detected in LGR-5 overexpressing KY-G1 cells. Non-adherent cultures of KY-G1 cells formed spherical shapes and most of the cells in the center survived intact, whereas KY-V2 cells formed irregular spheres and some of these had a necrotic area at the center (Fig. 1G).

Overexpression of LGR5 promotes HCC cell viability, enhances colony formation, and decreases cell motility

The rates of proliferation of KY-G1 and KY-V2 cells were identical until cell numbers reached a maximum, however, KY-G1 cells survived longer in overgrowth conditions (Fig. 2A). Substantial numbers of KY-G1 cells survived after two weeks in overgrowth culture, whereas KY-V2 cells detached from the surface of the dishes and only a small proportion of cells survived in over-growth culture (Fig. 2B). In addition, KY-G1 cells were more resistant to the toxicity of puromycin (Fig. 2C), and also formed soft agar colonies more efficiently than KY-V2 cells (Fig. 2D). The motility of the cells was measured by performing scratch tests on confluent cell cultures. Retardation of cell migration was observed as early as 5 h in KY-G1 cells (data not shown), and scratch scars were repaired more rapidly at 24 h in KY-V2 cell cultures than in KY-G1 cell cultures (Fig. 2E). The reduction ability of LGR5-overexpressing cells to migrate after scratch wound assay was also previously reported in colorectal carcinoma cell lines [10].

LGR5-overexpressing HCC cells forms nodular tumors with decreased infiltration and metastatic foci

To further evaluate the function of LGR5 in vivo, KY-G1 or KY-V2 cells were transplanted into the subcapsular region of the livers of NOG mice. KY-G1 cells formed tumors with trabecular pattern in the liver, while KY-V2 cells formed tumors with ill trabecular pattern (Fig. 3A a, b). Expression of LGR5-FL was detected in the tumors formed by KY-G1 cells but not in the tumors formed by KY-V2 cells (Fig. 3A a, b inserts). Reticulum staining showed a trabecular pattern in the KY-G1 tumors, whereas a solid pattern was observed in the KY-V2 tumors (Fig. 3A c, d). Infiltration into the vicinal muscle tissues was rare in the tumors formed by KY-G1 cells, but occasionally seen in the tumors formed by KY-V2 cells (Fig. 3A e, f). When KY-G1 cells were transplanted into the subcapsular region of the spleen, the number of metastatic foci in the liver, and the number of micrometastases into the portal veins was lower, compared with transplantation of KY-V2 cells (Fig. 3B a–c). In addition, tumors formed by KY-V2 cells showed a wider area of hemorrhagic necrosis compared with those formed by KY-G1 cells.

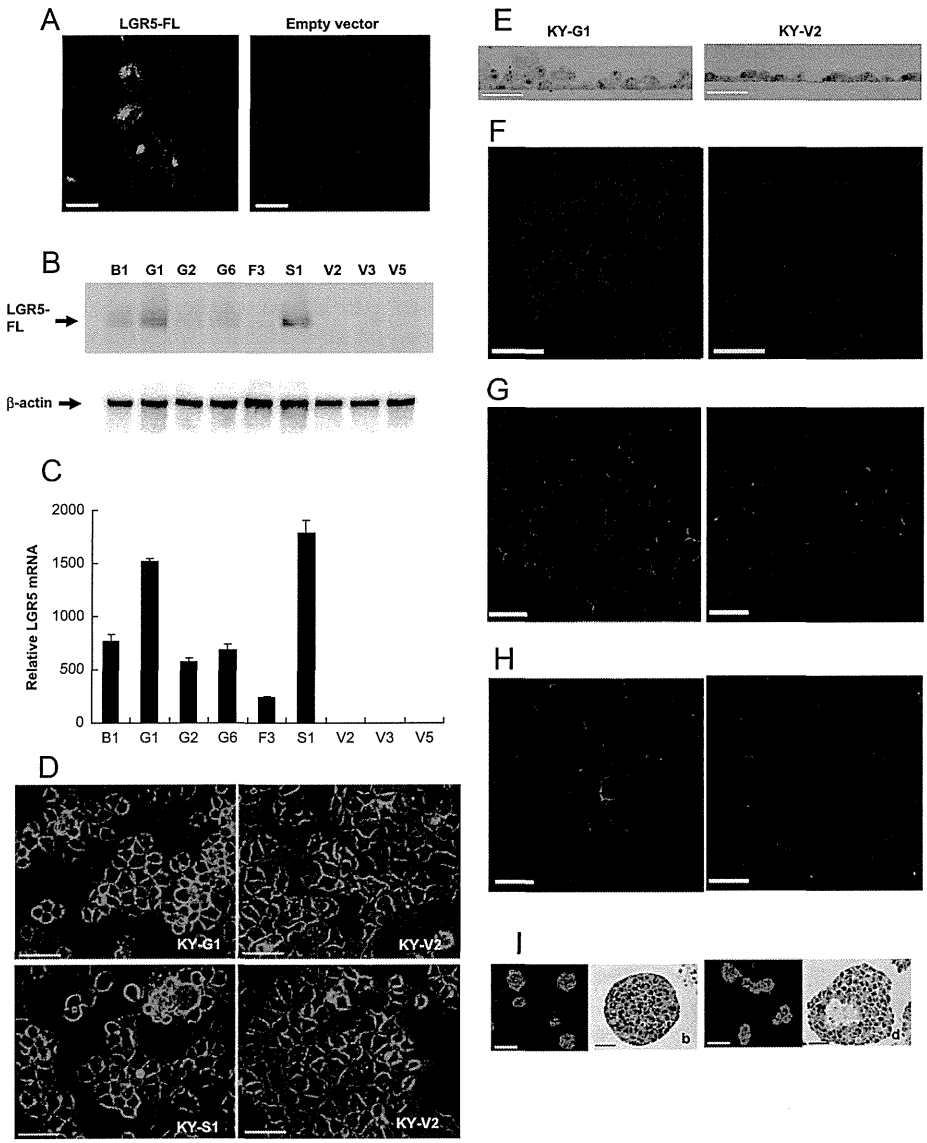

Fig. 1 – Establishment of LGR5-overexpressing clones. A: Immunofluorescent staining of KYN-2 cells transiently transfected with LGR5-FL or empty vector. Cells were stained with anti-FLAG antibody. Green: LGR5. Red: F-actin. Blue: nuclei. Bar, 50 μm. B: Western blot analysis of LGR5-overexpressing clones (KY-B1, KY-G1, KY-G2, KY-G6, KY-F3, KY-S1). KY-V2, KY-V3 and KY-V5 were stable transfectants containing empty vector. Blots were stained with anti-FLAG antibody (upper) or anti-β-actin antibody (lower). C: Expression of LGR5 mRNA in stable transfectants. Relative LGR5 mRNA level was shown as fold increase when the average level of non-transfected KYN-2 was set at 1. D: Morphology of clones containing LGR5-FL (KY-G1 and KY-S1) or empty vector (KY-V2 and KY-V3). (Bar, 100 μm) E: Vertical sections of 3-day cultures. KY-G1 and KY-V2 cells were embedded in EPON resin and sliced sections were stained with toluidine blue. F: Distribution of F-actin. F-actin was visualized by staining with phalloidin. Bar, 100 μm. G: Localization of E-cadherin (Green: E-cadherin, Blue: nuclei, Bar, 50 μm). H: Localization of β-catenin (Green: E-cadherin, Blue: nuclei, Bar, 50 μm). I: Morphology of non-adherent cultures of KY-G1 (a, b) and KY-V2 (c, d). Photographs show phase contrast microscopy (a, c. Bar, 200 μm) and HE staining of paraffin embedded sections (b, d. Bar, 500 μm). E-I: KY-G1 (left column), KY-V2 (right column). (For interpretation of the references to color in this figure, the reader is referred to the web version of this article.)

Down-regulation of LGR5 in HCC cells transforms cells to a loosely associated morphology and increased cell motility

To determine whether the characteristics of the KY-G1 cells were indeed due to the expression of higher levels of LGR5, we examined the effect of down-regulating LGR5 using siRNA. HepG2 cells were transfected with two siRNA sequences (si585 and si662) and LGR5 mRNA levels were analyzed by qPCR. LGR5 mRNA levels were significantly decreased 24–96 h after transfection of siRNAs against LGR5 (Supplementary Fig. 1; only 48 h data is shown). si662 suppressed expression of LGR5 more efficiently than si585, and similar results were obtained with

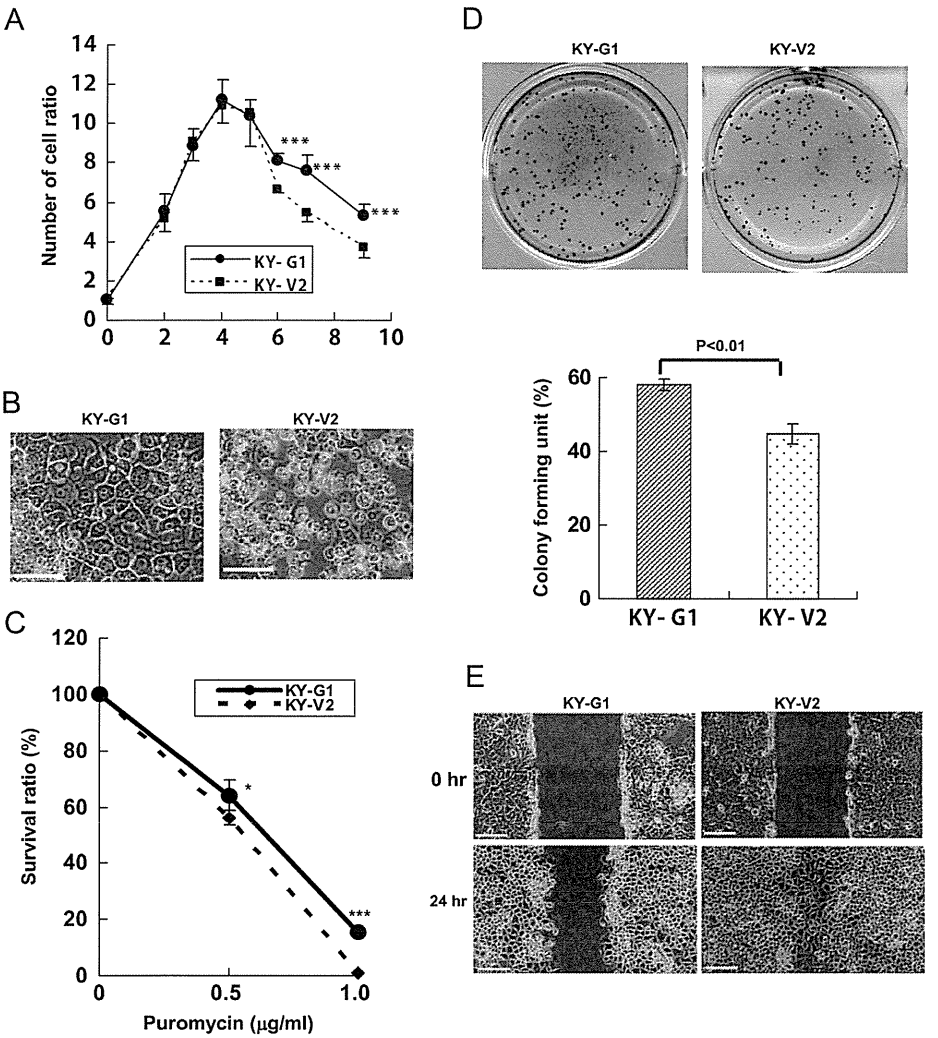

Fig. 2 – Characterization of LGR5-overexpressing clones. A: Growth and survival of KY-G1 and KY-V2 cells. High levels of LGR5 expression did not affect the growth rate of the cells; however, KY-G1 cells survived longer in overgrowth conditions. ***: $P<0.01$. B: Morphology of clones after 2 weeks of culture. (Bar, 100 μm) Viable cells were still observed in the KY-G1 culture, but few cells were alive in the KY-V2 culture. C: Resistance to cytotoxicity. Cells were treated with puromycin for 20 h, and cultured under soft agar medium. Cells with high expression of LGR5 were more resistant to the cytotoxic effect of puromycin. *: $P<0.05$. ***: $P<0.01$. D: Colony formation. Upper: 500 cells were cultured in soft agar plates for 2 weeks. Lower: quantitative assay of colony forming activity. Colony forming unit: ratio of colonies formed to number of cells inoculated (%). High levels of LGR5 expression enhanced colony formation. E: Motility assay. Confluent cell layers were scratched and photographed at 0 and 24 h. High levels of LGR5 expression inhibited cell motility. (Bar, 200 μm).

PLC/PRF/5 cells (Supplementary Fig. 2). When LGR5 mRNA was down-regulated with siRNA, the tight aggregated morphology of HepG2 cells was transformed to a loosely associated morphology. Some of the cells began to migrate away from the cell aggregates (Fig. 4A, upper column). The strongly staining cortical actins between the cells became extended filaments when expression of LGR5 was down-regulated (Fig. 4B, upper column). siRNA directed against LGR5 showed similar effects in PLC/PRF/5 cells (Fig. 4A and B, lower columns). The cortical actin between the cells became long, extended filaments. Down-regulation of LGR5 also increased cell motility. When HepG2 cells were treated with si585 or si662, scratched scars were repaired more rapidly than in cells treated with siControl (Fig. 5A, C). Similar results were obtained when PLC/PRF/5 cells were treated with siRNA directed against LGR5 (Fig. 5B, C).

Discussion

To determine the function of LGR5 in tumor cells, we carefully investigated cell clones containing a FLAG-tagged expression vector (LGR5-FL). The LGR-5 transfected clone (KY-G1) became rounded and formed aggregates when grown as an adherent culture. It formed spherical bodies when propagated in suspension culture, more resistance to cytocidal conditions, and showed decreased migratory activity. The Wnt signaling pathway is an

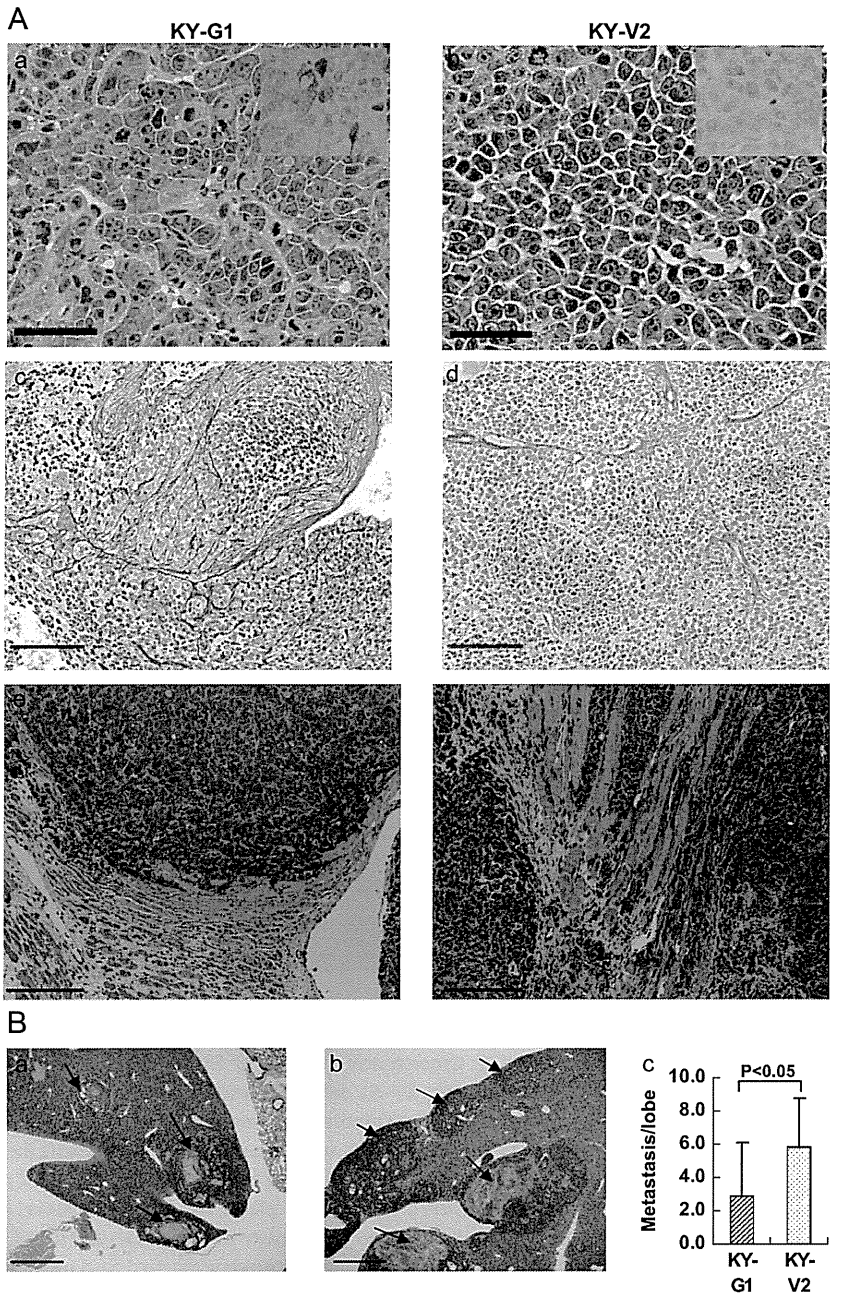

Fig. 3 – Histological analysis of tumors formed by KY-G1 or KY-V2 clones in the livers of NOG mice. A: KY-G1 (left) and KY-V2 (right) cells were transplanted into the subcapsular region of the livers of mice. Tumors were resected and thin sections were stained with HE (a, b. Bar, 100 μm)(e, f. Bar, 200 μm) or silver impregnation (c, d. Bar, 200 μm). Inserts show immunohistochemical staining with anti-FLAG antibody (a, b). B: KY-G1 (a) and KY-V2 (b) cells were transplanted into subcapsular region of the spleens of NOG mice. Tumors that formed in the livers were fixed and stained with HE (Bar 500 μm). Arrows show metastatic foci in the liver. The number of metastases was quantified (c). Tumors larger than 0.25 mm in diameter were counted. High levels of LGR5 expression inhibited metastasis to the liver.

important pathway for morphogenesis and maintaining the stemness of cells. Sphere formation, colony formation and resistance to cytotoxic drugs are important criteria for the stemness of cells. LGR5-overexpressing KY-G1 cells formed tightly packed spheres, with viable cells extending from the surface to the center when cultured under non-adherent conditions, whereas KY-V2 cells containing the empty vector formed loose, irregular spheres, and some cells in the central area showed signs of necrosis. KY-G1 cells were also more resistant to a cytocidal environment, survived longer under nutrient depletion conditions, and were more resistant to the cytocidal effect of puromycin. The differences between LGR5-transfected and vector-transfected cells were rather marginal, which may be affected by the

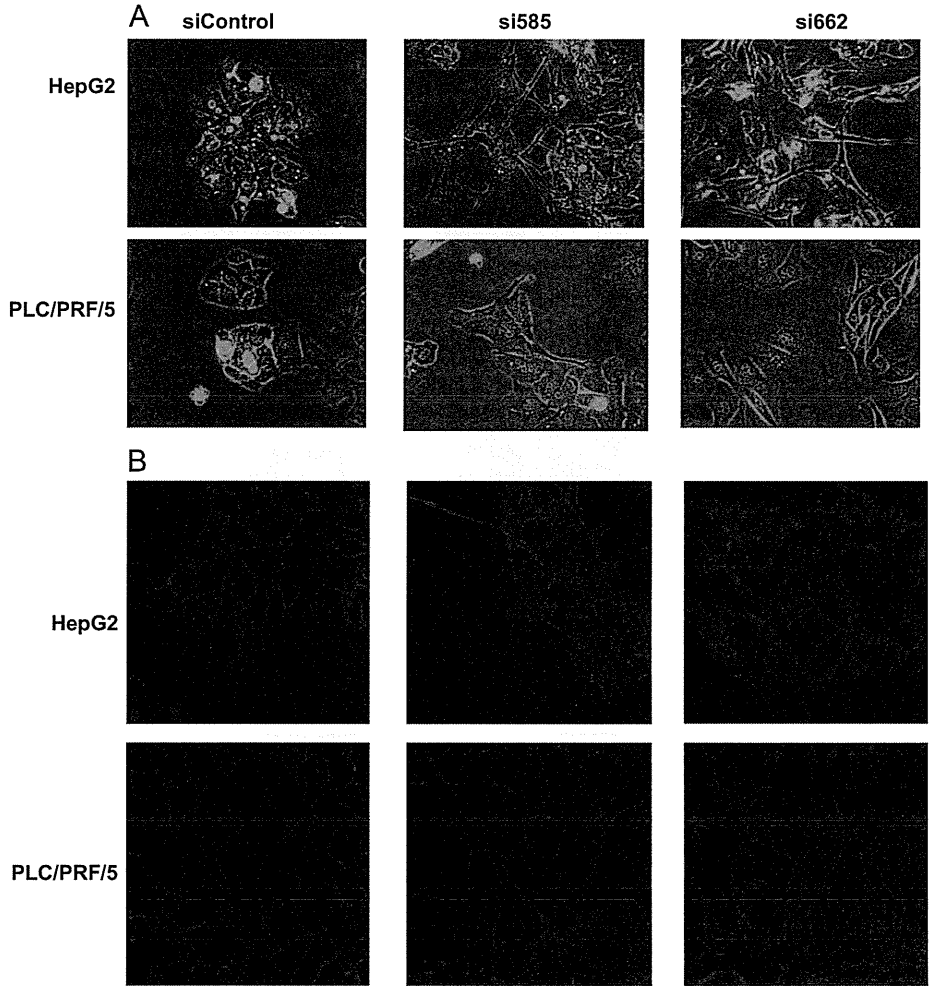

Fig. 4 – Down-regulation of LGR5 in HCC cell lines by treatment with siRNAs. HepG2 and PLC/PRF/5 cells were transfected with siControl, si585 or si662, and cultured for 2 days. A: Phase contrast microscopy. (×400) B: Immunofluorescent microscopy. Actin filaments were stained with phalloidin. (×400).

presence of substantial expression of LGR4 in parental KYN-2 cells. LGR4, LGR5, and LGR6 have homology with about 50% identity between each other at the amino acid level, and may compensate each other functions [18]. Since LGR4 is constitutively expressed in most kind of cells, we assumed that the results is more meaningful if we could obtain a difference between LGR5-overexpressing cells compared to the control empty vector cells, even though it is marginal. Moreover, we observed that parental KYN-2 cells had already reached the stage of anchorage-independent growth, while, a high level of LGR5 expression enhanced colony formation. This could be explained by high levels of LGR5 conferring resistance to cell death, and enhancing cell survival when they were scattered as single cells in the soft agar medium. KY-G1 cells aggregated and stacked up when cultured on the surface of the dishes, which consequently made them migrated slower than KY-V2 cells. These findings may explain why HCC is generally resistant to antitumor drugs used in chemotherapy. Many proteins related to the Wnt signaling pathway have been reported to modulate the actin–cytoskeleton structure. The frizzled/disheveled pathway controls the planar polarity of cells. Adenomatous polyposis coli (APC) protein is transported along microtubules, and regulates the cytoskeleton and cell migration [19]. β-catenin, a crucial transcription factor in the Wnt pathway, links E-cadherin with α-catenin to form firm adhesive junctions. LGR5, which is regarded as a target gene of the Wnt signaling pathway, quite possibly contributes to changes in cell morphology. Down-regulation of LGR5 in HepG2 and PLC/PRF/5 cells resulted in the cells acquiring a flat shape, with loss of cortical actin and migration of cells away from the aggregates. It also transformed HCC cells into a loosely associated morphology and increased cell motility. Reversely, high levels of LGR5 expression cells formed spherical shapes where most of the cells gathered intactly to the center. These results suggest that high levels of LGR5 expression affect epithelial cell morphology and confer some of the properties of stem cells on tumor cells.

To investigate the function of LGR5 in vivo, KY-G1 cells were orthotopically transplanted into NOG mice. KY-G1 cells formed nodular tumors typical of hepatocellular carcinomas, whereas the tumors formed by KY-V2 cells were diffuse and occasionally infiltrated into the contiguous tissues. Moreover, KY-V2 cells formed more micrometastases in the liver when implanted into the subcapsular region of the spleen. We previously categorized HCC cell lines into two groups; one highly metastatic and the